NUREG/CR-2323

Countercurrent Steam/Water Flow Above a Perforated Plate-Vertical Injection of Water

Prepared by I. Dilber, S. G. Bankoff, R. S. Tankin, M. C. Yuen

Department of Chemical Engineering
Department of Mechanical and Nuclear Engineering
Northwestern University

Prepared for
U.S. Nuclear Regulatory Commission

Available from

GPO Sales Program
Division of Technical Information and Document Control
U. S. Nuclear Regulatory Commission
Washington, D. C. 20555

Printed copy price: $3.75

and

National Technical Information Service
Springfield, Virginia 22161

NUREG/CR-2323
R2, R4

Countercurrent Steam/Water Flow Above a Perforated Plate-Vertical Injection of Water

Manuscript Completed: July 1981
Date Published: September 1981

Prepared by
I. Dilber, S. G. Bankoff, R. S. Tankin, M. C. Yuen

Department of Chemical Engineering
Department of Mechanical and Nuclear Engineering
Northwestern University
Evanston, IL 60201

Prepared for
Division of Accident Evaluation
Office of Nuclear Regulatory Research
U.S. Nuclear Regulatory Commission
Washington, D.C. 20555
NRC FIN B6188

ABSTRACT

Countercurrent flow limiting phenomenon above a perforated plate has been studied in a steam/water environment. Water was injected as a vertical jet and the injection height above the perforated plate was changed from 0 cm to 35.6 cm. The 15 hole perforated plate has a rectangular cross section with a perforation ratio of 0.423. The weep-points and total dumping points have been determined for low and high water injection heights above the perforated plate and the results have been compared to those of the horizontal water spray experiments. The data corresponding to high water injection heights were similar to those of the horizontal water spray experiments. However a different behavior was observed for the weep-point data with low water inlet heights. The dumping point was little affected by the water inlet position above the perforated plate. The dimensionless effective steam flow rate defined for the experiments with horizontal water spray was used to correlate the data corresponding to both the onset of weeping and the total dumping points. The correlation was successful for the weep-point data with high water injection heights. However the dimensionless parameter was redefined for the weeping-point data with low water injection heights. Assuming that the total dumping data corresponded to the point just before dumping occurred, the dimensionless water delivery rate was found to be independent of the inlet water flow rate. However it depended on the water inlet height above the perforated plate. When an unheated block with a perforation ratio of 0.254 was placed below the plate to simulate a heating core, choking occurred at the block instead of the plate. The block was then tested with a 9 hole plate having the same perforation ratio as the block, and with horizontal water

spray. The steam flow rates for weeping-point were found to be higher than those obtained without the block. It is thought to be due to both the change in steam velocity profile because of the presence of the block and the difference between the criteria used to determine the weep-point.

TABLE OF CONTENTS

LIST OF FIGURES AND TABLES

Figures

Table

NOMENCLATURE

A	Area
C	Empirical constant defined in Eq. (14)
C_p	Specific heat
D	Characteristic dimension, diameter
D^*	Bond number defined in Eq. (7)
f	Condensation efficiency (slope of $\dot{h}_g$ vs. $\dot{h}_p$ curve)
g	Acceleration due to gravity
h	Enthalpy
$\dot{h}$	Enthalpy flux
h_i	Water inlet position above the perforated plate
H^*	Dimensionless flux defined in Eq. (11)
I	Parameter defined in Eq. (27)
j	Volumetric flux (mass flow rate divided by density and open flow area through the plate)
J^*	Dimensionless flux defined in Eq. (2)
K	Kutateladze number defined in Eq. (5)
K^*	Turbulence constant
L^*	Bond number as defined in Eq. (15)
m	Empirical constant
n	Number of holes in Eq. 15); geometric similarity parameter in Eq. (24)
R_T	Thermodynamic ratio
T	Temperature
t_p	Thickness of the perforated plate
w	Characteristic dimension defined in Eq. (12)
W	Mass flow rate
α	Constant defined in Eq. (13)

$3\nabla T_{sc}$	Critical local subcooling
ρ	Density
σ	Surface tension

Subscripts

d	Delivery
e	Effective
f	Liquid phase
fg	Phase change
g	Vapor phase
h	Hole
i	Evaluation at intersection point in Eq. (26)
in	Inlet
ℓ	Liquid (water)
sat	Saturation condition
t	Total
v	Superheated vapor

1. Introduction

The flooding phenomena of countercurrent two phase flow have been studied in various types of flow channels since the early 50's. The former interest was in the performance of perforated plate in distillation towers or packed-bed chemical reactors (1,2). Recently, due to concern about the refilling and reflooding process in the event of a loss-of-coolant accident (LOCA) in nuclear reactor safety analysis, flooding phenomena in annuli or outside the fuel rod bundles have become of particular interest (3,4). In case of a boiling water reactor (BWR), one of the emergency core cooling systems (ECCS) is a core spray system which operates to sprinkle water over a core to remove decay heat under the loss of coolant condition. When water is sprayed, part of it evaporates in the fuel bundles and rises, causing a countercurrent flow against the falling water. As a result, flooding occurs either outside the fuel bundles or above the tie plates. Therefore, understanding of the flooding phenomenon above perforated plates is part of an important problem; namely, function of emergency core cooling systems in case of loss of coolant accident in nuclear reactors. Recently, some work has been done concerning restrictive effects of ascending air/steam on water flowing downward through a perforated plate. A horizontal spray has been used to inject the water (5).

In this present work, water is injected as a vertical jet, and the effects of the vertical water inertia on the flooding phenomenon above a perforated plate are studied in a steam environment. The results are then compared with those of the horizontal spray experiments. Furthermore, the core is simulated by an unheated block, in order to analyze the effects of changes in flow pattern due to the presence of the block.

It is observed that, if water injection (vertically) is close to the perforated plate, the phenomenon is quite different than that with a horizontal spray. A vertical water jet increases the condensation rate which results in higher steam flow rates at onset of weeping. The influence of the water inlet position is also observed in the non-dimensional analysis. Furthermore, when a block is placed below the perforated plate, it changes the flow pattern, and therefore affects the flooding phenomenon.

Throughout this study, the term weeping refers to the condition where the ascending steam flow rate is high enough to prevent almost all water from flowing through the plate. The point where water just ceases to flow through the plate is called the weep point. On the contrary, the condition where (the steam flow rate is so low that) all the inlet water commences to flow through the perforated plate is called "dumping".

2. Technical Background

2.1. Analysis of Air/Water Experiments

Since the early stages of two-phase flow investigations, air/water experiments were used to determine the important factors of the phenomenon. In this way, condensation effects of steam are eliminated. Later, the results can be corrected for condensation of steam. Mayfield (6), Arnold (7) and Zenz (8) separately observed that the superficial gas velocity through the holes, j_{gh}, is an important factor in the weeping phenomenon, as well as the water inlet position above the plate.

To correlate the data on weeping rate from perforated plates, many investigators (9,10) adapted Wallis' (11) model or its modifications (12). Based on the air/water data from round tubes, the equation is of the form:

$$J_g^{*2/(n+1)} + mJ_f^{*2/(n+1)} = C \qquad (1)$$

where m and C are empirical constants, and $J^*_{g,f}$ are defined as:

$$J^*_{g,f} = [\rho_{g,f} j^2_{g,f}/g\ D(\rho_f - \rho_g)]^{1/2} \qquad (2)$$

where ρ is density, j is the volumetric flux which is equal to the mass flow rate divided by the density and the open flow area, g is gravitational acceleration and D is a characteristic dimension. Subscripts g and f refer to gas and liquid phase respectively. The constant n in Eq. (1) depends on the scaling of the mixing length, and is 3.5 or 2.5. Usually it is assigned the intermediate value of 3. Then Eq. (1) becomes

$$J_g^{*\,1/2} + mJ_f^{*\,1/2} = C \qquad (3)$$

Wallis suggested the use of the tube diameter as the characteristic length. The choice of the characteristic length in Eq. (2) for applications to parallel-plate, large-size tubes, annulus, and fuel bundle geometries is uncertain (11,13,14,16). Also, Eq. (1) does not depend on surface tension effects, according to Wallis' suggestion. To correlate the BWR bundle CCFL data, it is proposed (10) to use the characteristic length $[\sigma/g(\rho_f - \rho_g)]^{1/2}$ which has been successfully used in boiling and two phase flow (11,15). Thus Eq. (3) becomes (16)

$$K_g^{1/2} + mK_f^{1/2} = C \tag{4}$$

where

$$K_{g,f} = \{\rho_{g,f} j_{g,f}^2 / [\sigma\, g(\rho_f - \rho_g)]^{1/2}\}^{1/2} \tag{5}$$

and σ is surface tension. The characteristic length used in Eq. (4) is similar to the horizontal wave length used in Taylor instability. In the case of no downward liquid flow, i.e., $K_f = 0$, Pushkina and Sorokin (12) found that K_g, the Kutateladze number, was equal to 3.2.

Essentially, K can be expressed in terms of J^*:

$$K = J^* D^{*\,1/2} \tag{6}$$

where

$$D^* = D[g(\rho_f - \rho_g)/\sigma]^{1/2} \tag{7}$$

which is sometimes called the Bond number. J^* scaling represents a balance between inertial forces in the gas and hydrostatic forces. The Kutateladze number expresses the balance between inertial forces in the gas, buoyancy forces and surface tension forces. It is particularly appropriate when no characteristic dimension of the apparatus is important (14). Wallis and Makkenchery (14) found that J^* scaling was appropriate for the limited range of D^* from 3 to 20, whereas K scaling was more appropriate for D^* larger than 30.

Looking back to Eq. (3) or Eq. (4), Wallis has established that the coefficient m equals unity for turbulent flow. This has been confirmed by data obtained in BWR or PWR tie plate geometries by Jones (9), Naitoh (17) and Jacoby (18). Hence, Eqs. (3) and (4) take the form

$$J_g^{*\,1/2} + J_f^{*\,1/2} = C \tag{8}$$

and

$$K_g^{1/2} + K_f^{1/2} = C \tag{9}$$

Since neither J^* scaling nor Kutateladze number covers the whole range of D^*, an intermediate scaling is suggested (5).

$$H_g^{*\,1/2} + H_f^{*\,1/2} = C \tag{10}$$

where

$$H_{f,g}^* = [\rho_{f,g}/gw(\rho_f - \rho_g)]^{1/2} j_{f,g} \tag{11}$$

and

$$w = D_h^{(1-\alpha)}[\sigma/g(\rho_f - \rho_g)]^{\alpha/2} \tag{12}$$

The constant α is defined as a hyperbolic tangential function:

$$\alpha = \tanh\left[\frac{2\pi D_h}{t_p}(A_h/A_t)\right] \tag{13}$$

where A_h/A_t is the perforation ratio, D_h is the hole diameter and t_p is the plate thickness. Thus the value of α changes between zero and one. For α equal to one, H^* scaling is identical to K scaling. On the other hand, for α equal to zero, Eq. (10) reduces to J^* scaling. When α takes values between zero and one, H^* scaling results in a smooth transition between the two models.

A correlation of the coefficient C in terms of the Bond number L^*, is given by Hsieh (5) as:

$$C = 1.07 + 4.33 \times 10^{-3} L^* \tag{14}$$

where

$$L^* = n\pi D_h[g(\rho_f - \rho_g)/\sigma]^{1/2} \tag{15}$$

It is noted that Eq. (10) is applicable for the range $30 < L^* < 200$.

Thus, the weeping rate for perforated plate can be predicted by using the equation

$$H_g^{*\,1/2}/C + H_f^{*\,1/2}/C = 1 \qquad (16)$$

where C is given by Eq. (14).

2.2. Analysis of Steam/Water Experiments

The thermodynamic ratio, R_T, defined as:

$$R_T = C_p(T_{sat} - T_f)W_f/h_{fg}W_g \qquad (17)$$

is adopted as the main parameter in characterizing the performance of condensation driven two-phase flow systems. For direct contact condensation, the line $R_T = 1$ separates the universal flow regime into two-major regions. Complete condensation is possible in the region $R_T > 1$.

But recent experiments reveal that the thermodynamic boundary, $R_T = 1$ line, does not predict the performance of the flow regime in annuli or perforated plate geometries. In addition to that, a hydrodynamic boundary which can be expressed in the form of Eq. (16), is observed in the region $R_T < 1$. The flow regime, here, is analysed using the steam and water enthalpy rates, $\dot{h}_g$ and $\dot{h}_\ell$ respectively. They are defined as:

$$\dot{h}_g = W_g h_{fg} \qquad (18)$$

$$\dot{h}_\ell = W_f C_p(T_{sat} - T_f) \qquad (19)$$

where W_g and W_f are the steam and water mass flow rates, respectively; h_{fg} is the evaporation enthalpy of steam; C_p specific heat; T_{sat} saturation temperature; and T_f water inlet temperature. The steam enthalpy rate was further corrected for slight superheat temperatures, h_{fg} was replaced by $h_{vf} = h_v - h_f$ where h_v is the steam enthalpy and h_f is the saturated liquid enthalpy.

The non-dimensional scalings that are defined for air/water media can be corrected for condensation effects. The J^* scaling defined in Eq. (3) can be expressed as (3,19):

$$\{J^*_{g,c} - f[(T_{sat} - T_f)C_p/h_{fg}](\rho_f/\rho_g)^{1/2} J^*_{f,in}\}^{1/2} + mJ^{*\,1/2}_{f,d} = C \quad (20)$$

where f is the condensation factor, and is obtained empirically. $J^*_{f,in}$ and $J^*_{f,d}$ are non-dimensional water inlet and delivery rates, respectively, and $J^*_{g,c}$ is the non-dimensional gas flow rate, as defined in Eq. (2).

Similarly, the H^* scaling can be corrected for condensation effects by defining the non-dimensional effective steam flow rate as:

$$H^*_{g,e} = H^*_g - f[C_p(T_{sat} - T_f)/h_{fg}](\rho_f/\rho_g)^{1/2} H^*_{f,in} \quad (21)$$

where the mixing efficiency, f, is taken to be the slope of $\dot{n}_g$ vs. $\dot{n}_\ell$ curve. Then, the flooding equation suggested for air/water experiments in Eq. (10) becomes:

$$H^{*\,1/2}_{g,e}/C + H^{*\,1/2}_{f}/C = 1 \quad (22)$$

At the weep point, where there is no water delivery through the holes, Eq. (22) becomes:

$$H_{g,e}^{*\,1/2}/C = 1 \qquad (23)$$

where C is given in Eq. (14).

Eq. (23) is used to correlate the weep point data. The coefficient f is calculated separately for each set of data, because it is observed that f is a function of water inlet position. Furthermore, the effective steam flow rate, $H_{g,e}^{*}$, is also used to interpret the dumping data. It was shown (5) that, $H_{g,e}^{*}$ successfully correlated steam/water data for high water inlet position, and horizontal water spray configuration. But no correlation was available for low injection points and/or vertical water jet configuration.

Currently, some work is being done at Northwestern University to analyze the effect of a block below the perforated plate on the weeping phenomenon. The block affects weeping by changing the steam flow pattern upstream of the perforated plates. It may be desirable to use a heated block below the perforated plate and thus determine the effect of heat transfer on weeping.

3. Apparatus, Procedure and Visual Observations

3.1. Vertical Water Jet Experiments

3.1.1. Test Channel

The channel shown in Fig. 1 consists of a brass frame, the test plate and the Lexan walls. The frame consists of side walls and the top and bottom plates, and is made of 12.7 mm thick brass. The front and back sides of the frames are covered with 3/4" thick Lexan plates in order to provide visual observations. Each Lexan wall is made of three pieces and their connections are reinforced by brass plates which help prevent the leakage and also prevent the frame from bending.

The 15 hole plate that C. Hsieh (5) used for horizontal jet experiments, was used for vertical jet experiments. It is made of brass and is similar to the German KWU PWR fuel assembly lower tie plate geometry (Fig 2). The plate has a perforation ratio of 0.423 and can be placed either 267 mm or 445 mm below the water overflow port. Since it has been observed that this distance does not have much effect on the weeping phenomenon (5), the plate was kept at 267 mm.

3.1.2. Water and Steam Lines

Water from the building line goes through two rotameters placed in parallel. The outputs of the rotameters are both connected to a 1/2" OD brass tube with a flexible hose. The brass tube enters the test section through the top. The water inlet position above the test plate can be adjusted by moving the tube up and down. The water jet is always vertically downward.

Steam from the building line first passes through either a 1 1/4 or 2" venturi, then through a heater. After that the steam line is divided into two 1" pipes which lead to the steam inlets placed on each side of the channel.

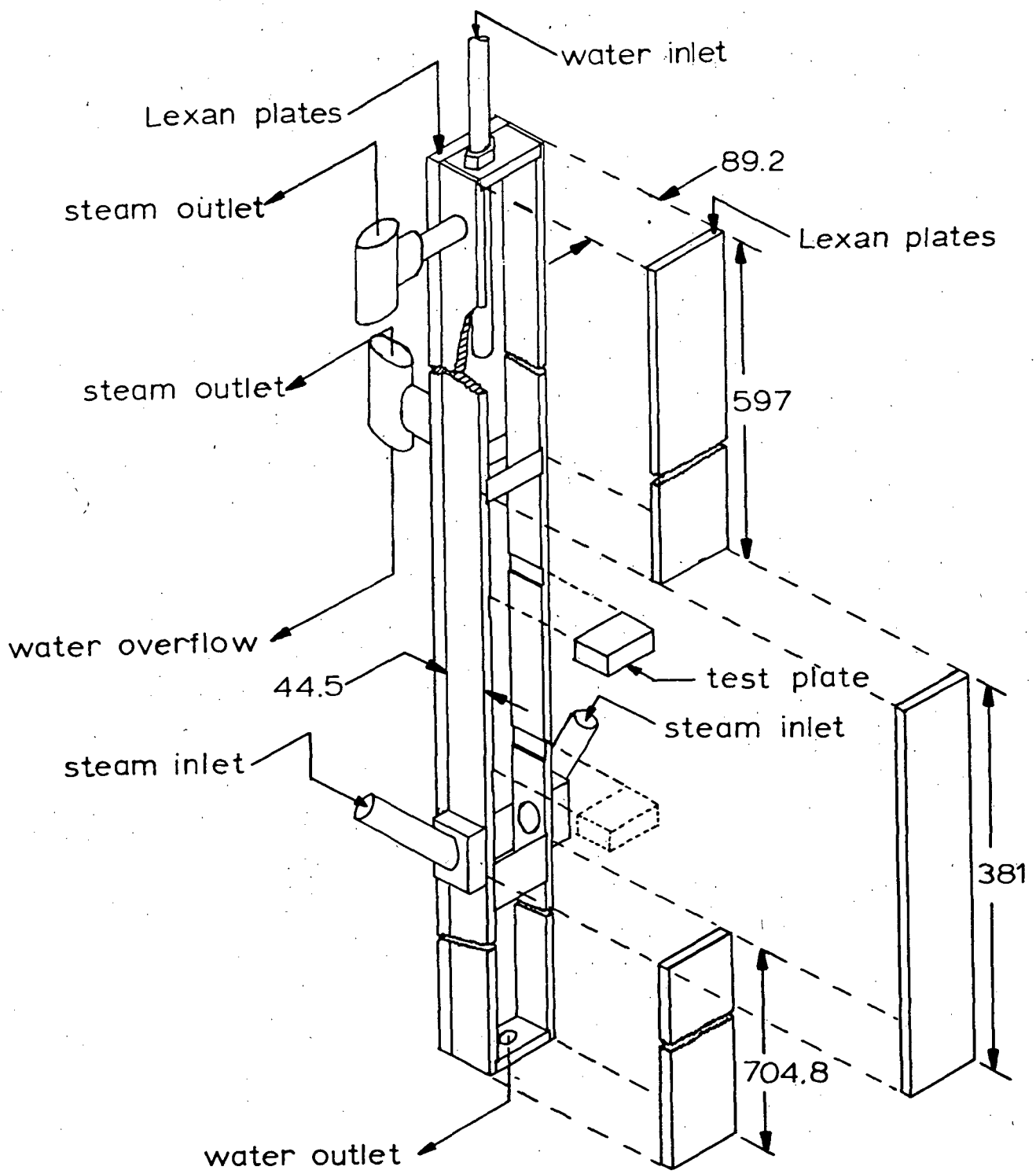

Fig. 1 The test channel (dimensions in mm)

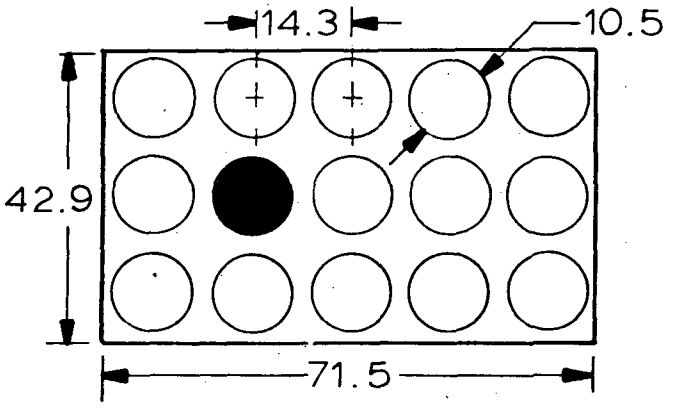

a. 15 hole plate

plate thickness 20 mm

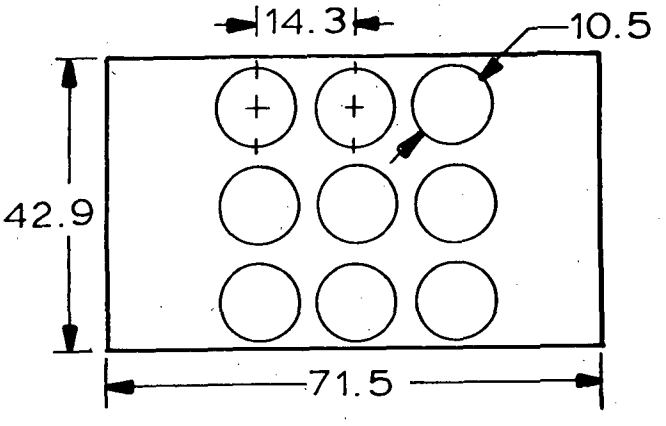

b. 9 hole plate

Fig. 2 The perforated plates.

The steam inlet pipes are at 45 ^{o} angle with the channel sides, pointing downward, in order to minimize the entrance effects and to get a fairly uniform flow in the neighborhood of the test plate.

Water trapped above the test plate flows out of the test section through a 50 mm overflow port at the back of the channel. This water passes through a pyrex tee that functions like a water steam separator. The water weeping from the perforated plate is collected at the bottom of the channel and can be taken out by the water outlet attached to the bottom of the channel. The amount of steam that is not condensed in the channel can flow out either from the water overflow port, which then is separated from the water at the pyrex tee, or from the steam outlet near the top of the channel. A schematic view of the test channel is shown in Fig. 3, together with the steam and water lines. The locations of thermocouples and pressure transducers are also shown and their functions are listed in Table 1.

3.1.3. Instrumentation

The rotameters used in the water line are both scaled from 5 to 50 pounds per minute, which, when calibrated, corresponds to .0407 kg/sec to .416 kg/sec for one and .0264 kg/sec to .279 kg/sec for the other.

A differential pressure transducer is used to measure the pressure difference in either 1 1/4 or 2" steam venturi. The absolute pressure and the temperature at the venturi are also measured in order to determine the properties of the steam. Then these data are used to calculate the steam flow rate.

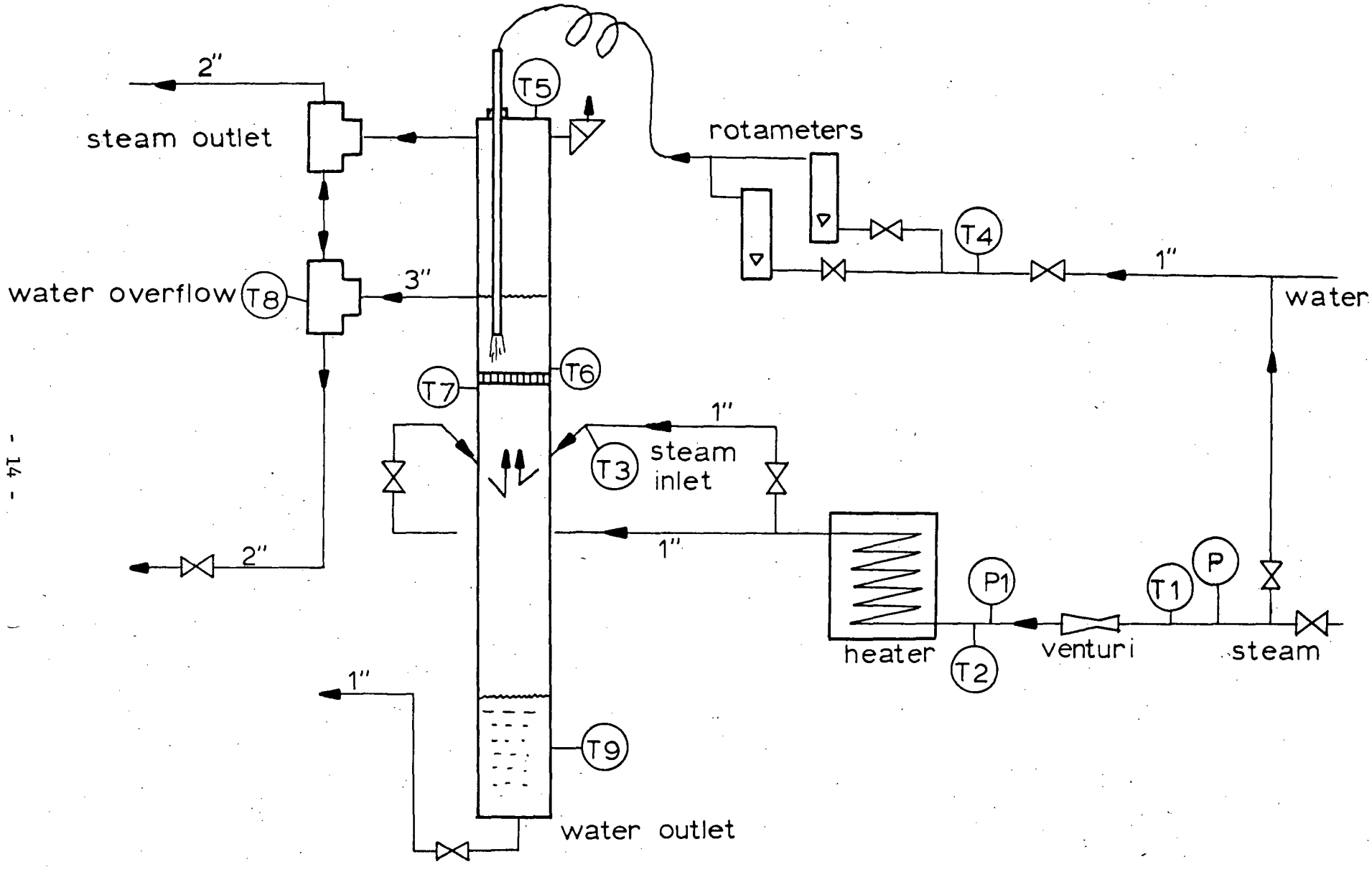

Fig. 3 Schematic diagram of the test channel and steam and water lines.

TABLE 1

Functions of Various Thermocouples and Pressure Transducers

(Refer to Fig. 3)

T1: Temperature of Steam at 1 1/4" or 2" Venturi

T2: Temperature of Steam at the Heater Inlet

T3: Steam Inlet Temperature

T4: Water Inlet Temperature

T5: Temperature at the Top of the Channel

T6: Temperature Above the Plate

T7: Temperature Below the Plate

T8: Outlet Water Temperature

T9: Temperature of Water accumulated at the Bottom of Channel

P : Absolute and Differential Pressures of Steam at Venturi

P1: Absolute Pressure of Steam at Heater Inlet.

The thermocouple readings that are necessary for the calculations measure water inlet, steam inlet, and water outlet temperatures. The other readings are also recorded, but they do not appear in primary calculations; they are kept as a reference.

3.1.4. Experimental Procedure and Visual Observations

During the period of the experiments, the inlet water temperature varied from 0 ^{o}to 12 ^{o}C. The pressure inside the channel was maintained about atmospheric pressure, and the inlet steam was saturated. The position of water inlet above the plate was changed from 0 cm to 35.6 cm; the jet was always downward toward the shaded hole in Fig. 2a., such that, at least 90% of the jet would pass through that hole. The one exception was the 0mm data, when the water inlet tube was attached to the center hole.

In order to determine the weep point, first the desired water flow rate is set, the water outlet at the bottom of the channel being open so that the water level inside the channel can be controlled. Then the steam flow rate is increased until the weep point is reached. In horizontal jet experiments the weep point was defined as the condition where there is no water flow through the perforated plate. But in the case of vertical water jet, this criterion cannot be used, especially for water injections near the plate. Due to high water inertia, the steam flow rate cannot prevent the jet from passing through the plate. Hence, there is always some water flowing through the hole in the plate which is then blown up in a neighboring hole in the perforated plate by the steam flow. Due to this fact, the criterion used for horizontal jet injection is not applicable to vertical jet injection. Instead, the weep point was determined by monitoring the level of the water at the bottom of the channel. Since the amount of steam condensed, due to contact with water at

the bottom of the test section, is negligible (this water is at saturated temperature), when a slight increase of the water level is observed, it is assumed that the weep point is reached. The amount of water causing the level to increase was always confined to a few percent of the inlet water flow rate. In order to be consistent, the same criterion was used for high water injection heights where there is no jet of water through the plate prior to weeping.

No weeping experiments were also run by setting the steam first and then adjusting the water flow rate. No major differences were observed in the resulting data.

In the case of dumping data, first a partial delivery state is reached. Then, either the water flow rate is increased or the steam flow rate is decreased until all the water above the test plate comes down suddenly. For some flow rates, the dumping phenomenon is not stable. That is, after dumping occurs, water is blocked by the steam below the plate, then it is blown up above the plate, and the process repeats itself. This sequence may continue. However sometimes, usually after the first few dumpings, no further blockage of water is observed, and the sequence ends. In this case water flows down as a jet, and the steam flows up around it without any disturbance.

When the steam flow rate is slowly increased from zero while water is flowing inside the channel, it has been observed that, first, the water jet becomes unstable near the steam inlet. Then, a further increase of steam flow rate results in breaking down of the jet. Some water droplets are formed near the steam inlet region, but they are quickly blown up above the plate. Thus, there is a sudden change from total delivery to partial delivery.

At the weep point, with water inlet at 0 or 50 mm above the perforated plate, the jet passing through the test plate is turned up in a U pattern

switching from hole to hole around the injection hole. When the water inlet is at 203 or 356 mm above the perforated plate, there is no water jet flowing through the plate, but from time to time, there are some water drops flowing down. These drops are blown up by oncoming steam flow.

For low water flow rates, the pool above the plate is a fully turbulent two phase flow (steam escapes from the water surface). As the equilibrium is reached with higher water flow rates, total condensation occurs within the pool. The two phase region becoming smaller with higher water flow rate. As the flow rates are further increased, the whole pool above the plate becomes unstable and starts to oscillate up and down, even penetrating the perforated plate from time to time. For the highest water flow rates tested, total condensation was confined to the neighborhood of the perforated plate.

3.2. Experiments with Unheated Block Below Perforated Plate

3.2.1. Test Channel

The channel design has been slightly changed (designed by C. L. Chen) for the analysis of weeping phenomenon with a block below the perforated plate. In this study, an unheated block has been used to analyze the effect of the change in steam flow pattern due to the presence of the block.

Instead of the Lexan walls, pyrex glass has been used. Instead of the water overflow port at the back of the channel, two 1" pipes have been attached 12" above the test plate, on each side of the channel. The water outlet at the bottom of the channel has been also moved to the sides, similar to the overflow outlet. The steam inlets were moved 254 cm below its original position, but still pointing downward at a 45 ^{o}angle.

The unheated block, which is made of brass, is 15.24 cm long. This is assumed to be sufficient length for the flow to be established. The hole configuration of the block is shown in Fig. 4. The cross section was designed such that the ratio of the flow area to the total cross section of the channel is about the same as the perforation ratio of a 9 hole plate (Fig. 2b.).

3.2.2. Experimental Procedure and Visual Observations

The 15 hole plate has been used with the vertical water jet to analyze the effect of the block, placed either 1.9 cm or 5.7 cm below the plate. Water inlet positions tested are 5 cm and 20.3 cm above the plate. The same criterion as in the previous experiments was used to determine the weep point.

In order to prevent large oscillations at the start of the experiments, it is preferred to adjust first the steam flow rate. Then the water flow rate is adjusted until water drops start to reach the bottom of the channel. The water jet passing through the plate breaks up on hitting the block. At high water flow rates, choking occurs at the block, instead of the perforated plate. It is also observed that the flow is much more unstable than without the block. Even the water column at the bottom of the channel is disturbed and carried away due to large oscillations. This description applies to the vertical injection of water.

The 9 hole plate (Fig. 2b) with a perforation ratio of 0.254 and the horizontal water injection tube of C. L. Hsieh (5) are used to study the effect of the flow pattern due to the presence of the block. A horizontal jet is more suitable for the analysis, because it does not involve inertial effects. The results can be compared to those of Hsieh's (5), which were also obtained with horizontal water injection and 9 hole plate, but without the block. The weep point is determined by visual observations only. There were

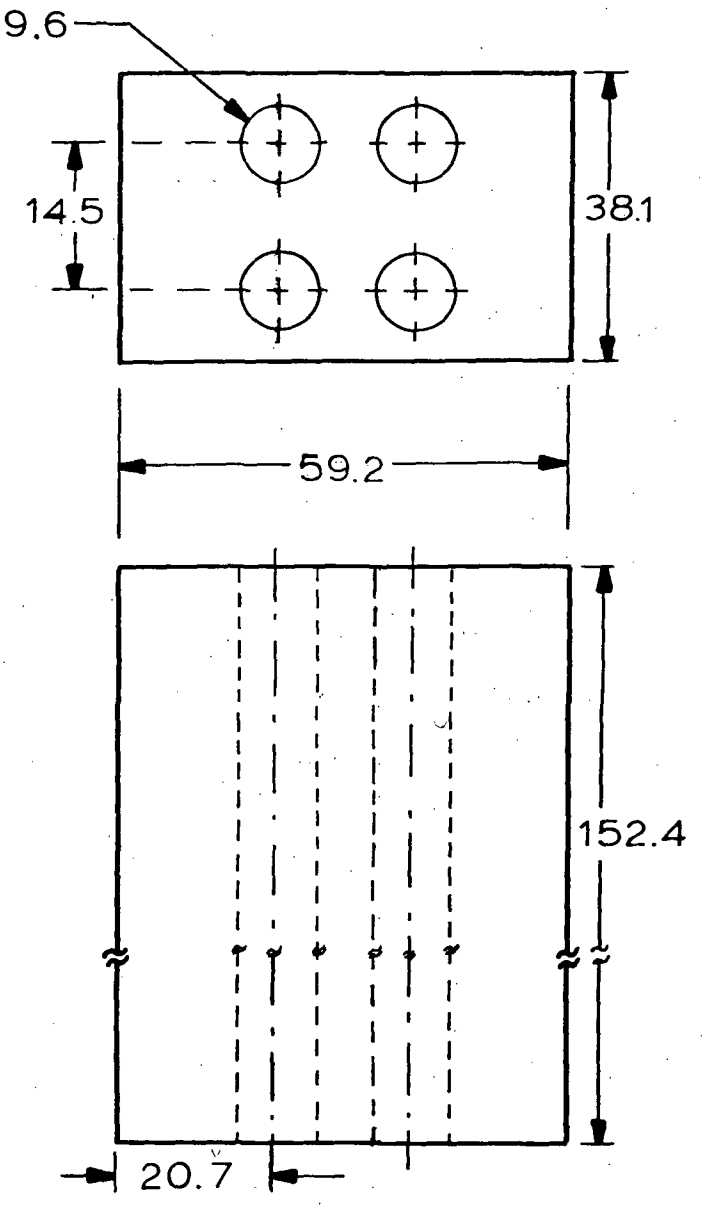

Fig. 4 The block used for the simulation of a heating core.

no water drops below the perforated plate. Since there is no vertical water inertia, even for very low injection positions, it is possible to prevent water from flowing down the plate. Two different water inlet positions, namely 20.3 cm and 35.5 cm above the plate, have been tested with the block 5.7 cm. below the perforated plate. In this case, the flow is much smoother than the vertical injection experiments. Furthermore the two-phase region is observed to cover the whole region between the plate and the water inlet, for almost all flow rates. Due to the geometry of the perforated plate, water accumulated near the walls of the channel, confining the two-phase region above the perforated region of the plate and below the water inlet.

4. Results and Discussion

4.1. Vertical Water Injection Experiments

4.1.1. Effect of Water Inlet Position Above the Test Plate

Four different water inlet positions were tested with vertical water jet and 15 hole plate; namely, 35.5, 20.3, 5.1, and 0 cm above the perforated plate. Since water temperature was between $0^{o}C$ and $12^{o}C$ and the steam temperature was approximately $100^{o}C$, temperature effects were neglected and the position of water inlet, h_i, was assumed to be the only parameter. The water injector was a 1/2"OD copper tube used throughout this set of experiments.

The weep point and the dumping point data for h_i equal to 35.5 and 20.3 cm are plotted in Fig. 5. No significant difference is observed for the weep point data. As for the dumping point data, the two curves differ slightly for high water enthalpy flux. It has been visually observed that, for high water flow rates, the region between the overflow port and the perforated plate is, more or less, a clear water pool. This is especially true for the dumping experiments where total condensation occurs, most of the time, at the plate. Because of the function of the water pool as a buffer, the momentum of the injected water cannot extend to the plate. This seems to be true for the weep point data at these two injection heights and agrees with Naitoh's (17) findings. But there must be another factor that causes a difference in the dumping data for the two inlet positions. One expects that the jet would get closer to the plate as the water inlet is lowered, and/or the flow rate is increased. Thus, for h_i= 30.3 cm., (the jet being closer to the plate) more cold water can reach the perforated plate, causing higher condensation rate. Therefore, in order to compensate for greater condensation, more steam is required. In the case of weeping data, the steam flow rate is high enough to

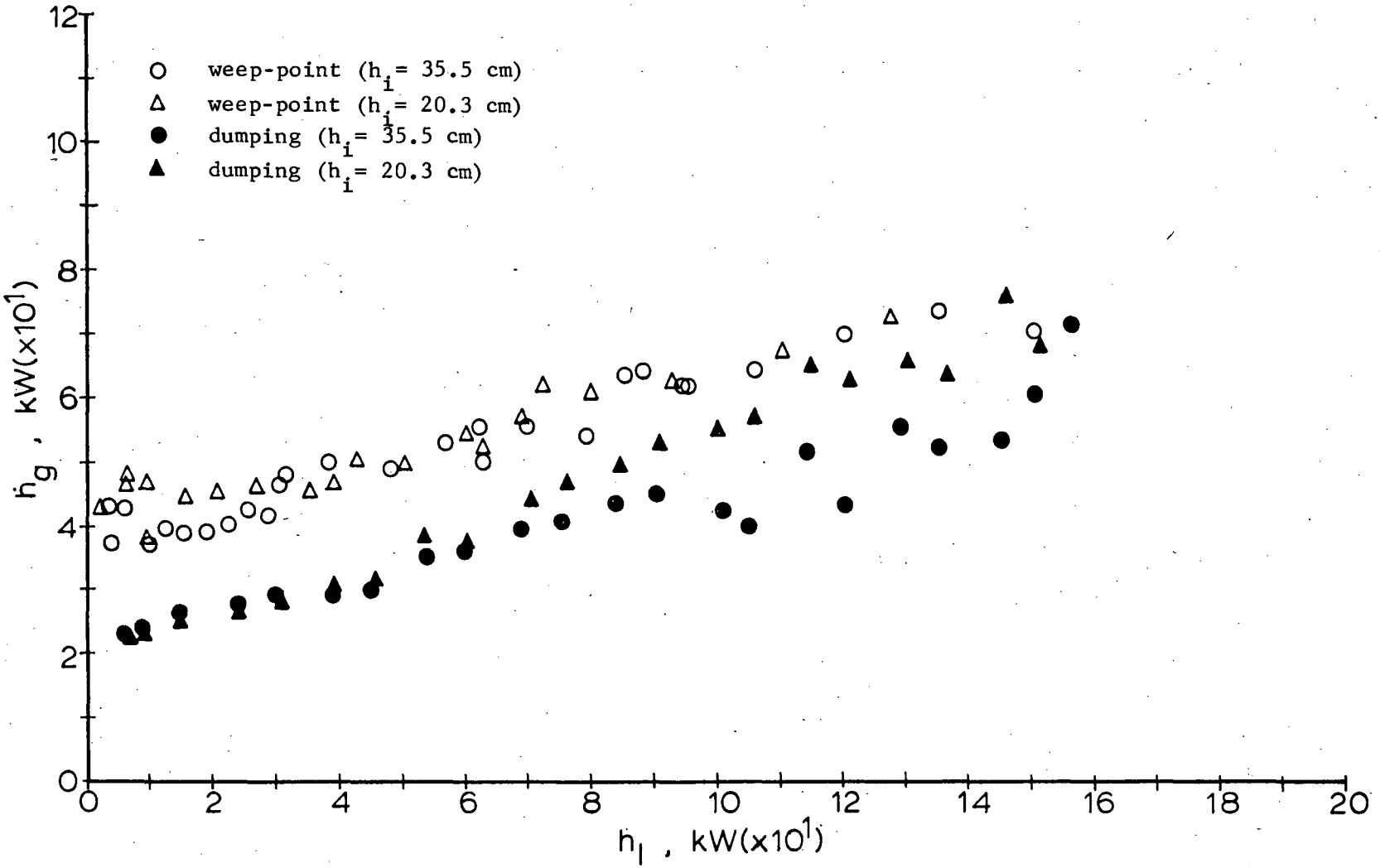

Fig. 5 High injection height data for vertical jet.

keep the pool temperature near the saturation point. Hence, the "effective length" of the jet includes both the inertial and thermal effects of the water jet.

Comparison of the 35.5 cm injection data with Hsieh's (5) 30.5 cm horizontal spray data reveals that the vertical inertia of the jet has no effect on the flooding data (Fig. 6). This indicates that the effective jet length cannot extend to the plate for 35.5 cm and 20.3 cm weep-point experiments.

A slight increase in slope of enthalpy flux curve was observed by Hsieh (5) for horizontal water spray placed at .5 cm above the plate. But the behavior of the curve is quite different for vertical water jet data with h_i = 5cm (Fig. 7) and below. Although the intercept is about the same as that of Fig. 5 for the weep point data, the slope is much higher in this case, for $\dot{h}_\ell$ < 50 KW. On the other hand, for $\dot{h}_\ell$ > 50 KW, the curve has a less steep slope. The higher value of the slope can be related to the visual observations. Now that the injection point is closer to the plate, the effective length of the jet reaches the plate and furthermore, the vertical inertia of the jet is so great that the ascending steam flow cannot prevent the jet from passing through the hole of the perforated plate. Therefore, some part of the steam is condensed before reaching the perforated plate, which necessitates the use of higher steam flow rate for the same water flow rate. On the other hand, because of the higher jet efficiency, more cold water is present just above the plate. This means a higher condensation rate at the perforated plate. Thus, the overall condensation efficiency is increased due to the presence of both the jet below the perforated plate and the cold water above the perforated plate. This is true until a saturated mixing condition is achieved. Then, condensation rate having reached a maximum, the slope of the

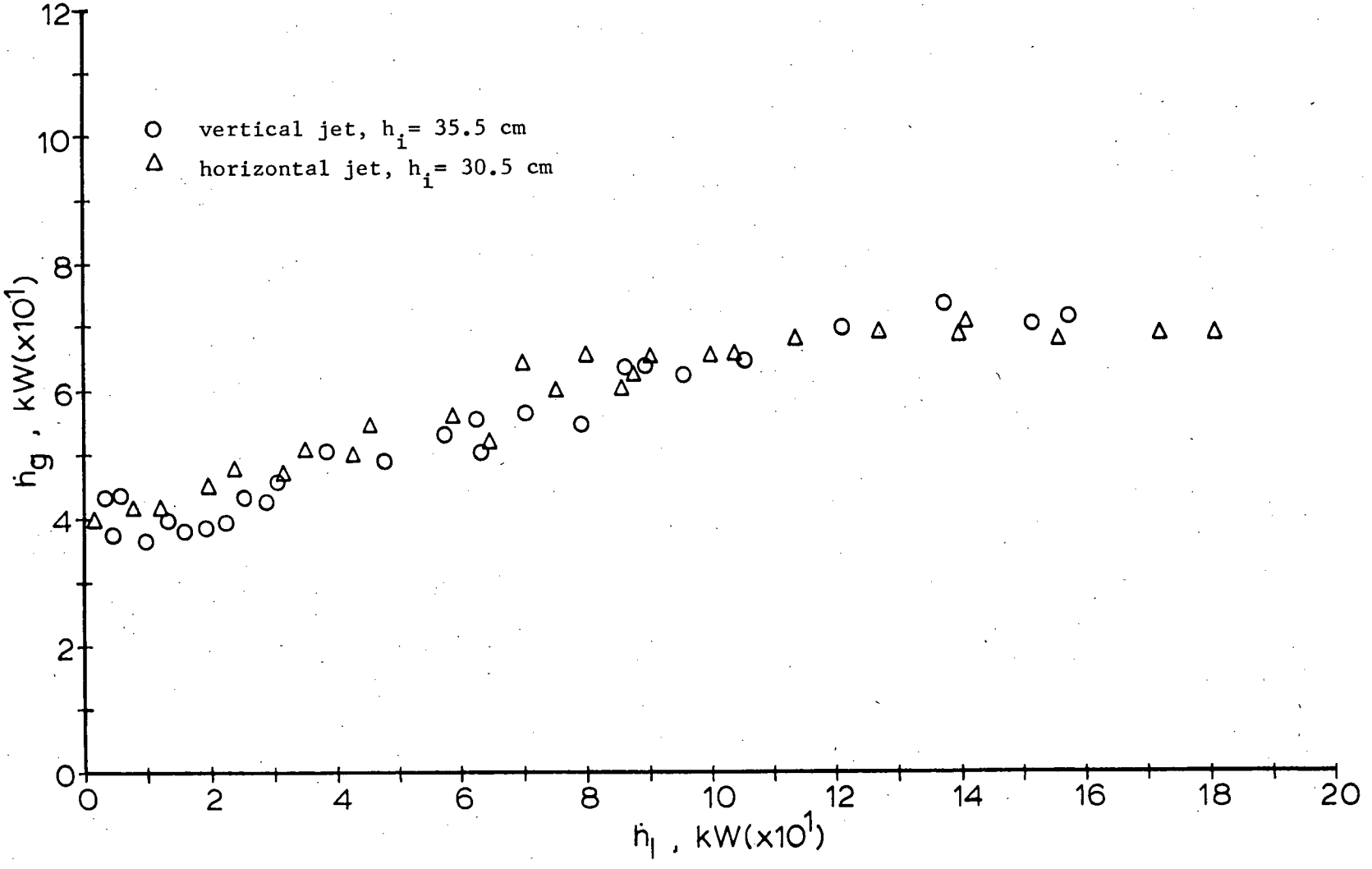

Fig. 6 Comparison of vertical and horizontal jet data, for high injection height.

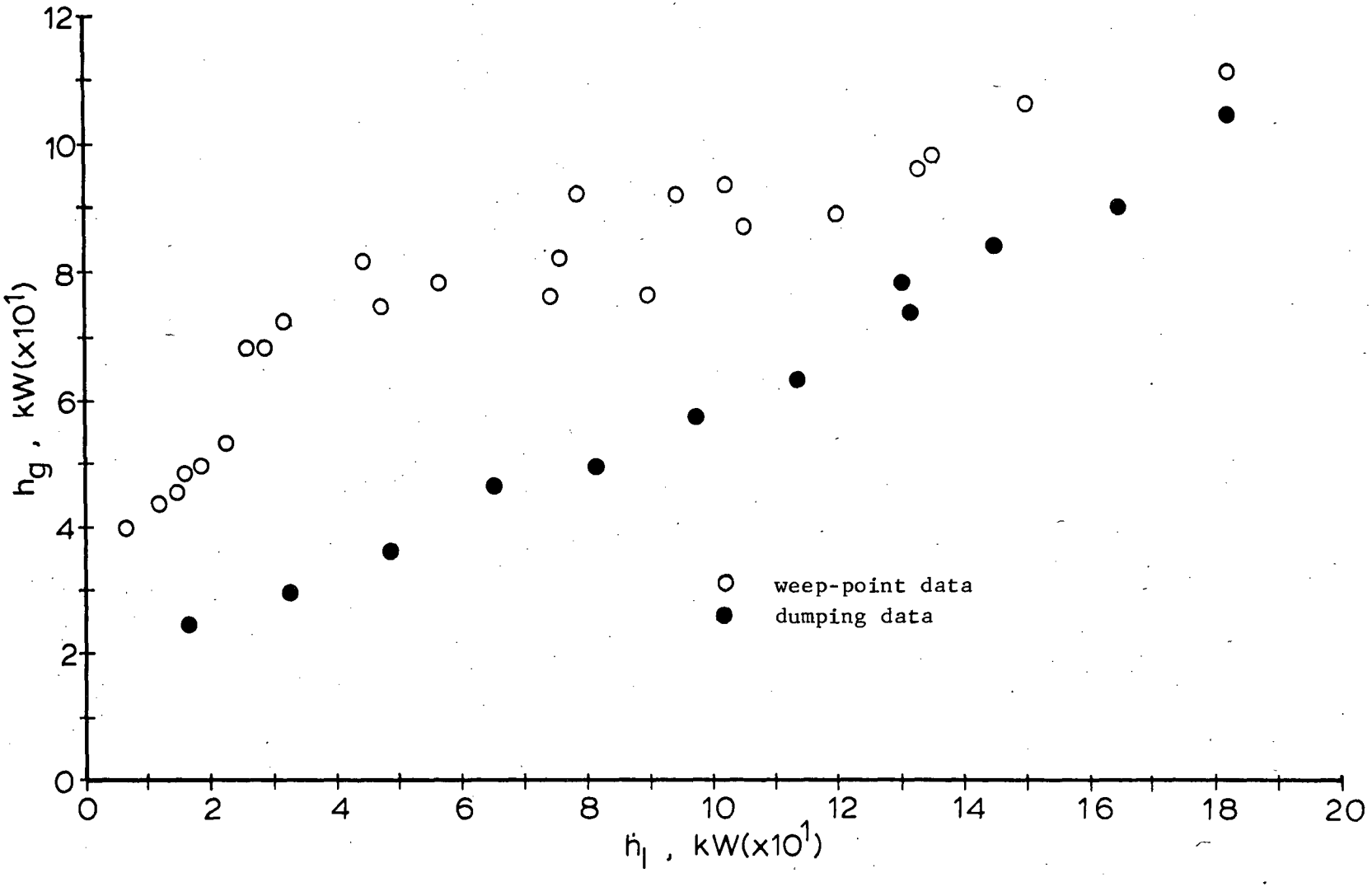

Fig. 7 Weeping and dumping data for vertical jet, h_i= 5 cm.

curve decreases, and further increase of water flow rate does not contribute much to condensation, but instead it is carried away from the overflow port. The change in slope of enthalpy flux curve was also observed for horizontal spray data (5). But in that case, the second part of the curve had zero slope. The small value of the slope in this case is thought to be due to the condensation of steam at the perforated plate. This can also be the cause of the slight increase in the slope of dumping data. The scatter in the weep point data is due to the unstable and oscillatory condition of the experiments. A comparison of the horizontal spray data for h_i = 10.1 cm with the vertical spray data for h_i = 5.1 cm and h_i = 20.3 cm is shown in Fig. 8. The horizontal spray data are the same as 20.3 cm vertical spray data.

As an extreme case, the water injection was brought to the plate by attaching the nozzle to the center hole of the plate. The results are shown in Fig. 9 together with horizontal spray data corresponding to a water inlet position 0.5 cm above the plate. The respective intercepts of the weeping and dumping curves are again unchanged, with respect to the previous data. The slope of the dumping curve is slightly higher than the corresponding curve for 5.1 cm injection. Furthermore, it coincides more or less with the weep-point data for horizontal spray. It can be thought that changing from horizontal spray to vertical spray very close to the plate would switch the flooding condition from weep-point to dumping. On the other hand, observation of the weep-point data reveals that the curve starts with a slope equal to one. This means that maximum condensation efficiency is reached in that particular region. Later, the slope decreases, but for $\dot{h}_\ell$ around 60KW and for much higher steam enthalpy flux, $\dot{h}_g$. This is also an expected result, since the full length of the vertical spray is now exposed to the oncoming steam below the plate. Therefore, most of the condensation occurs below the plate. It is

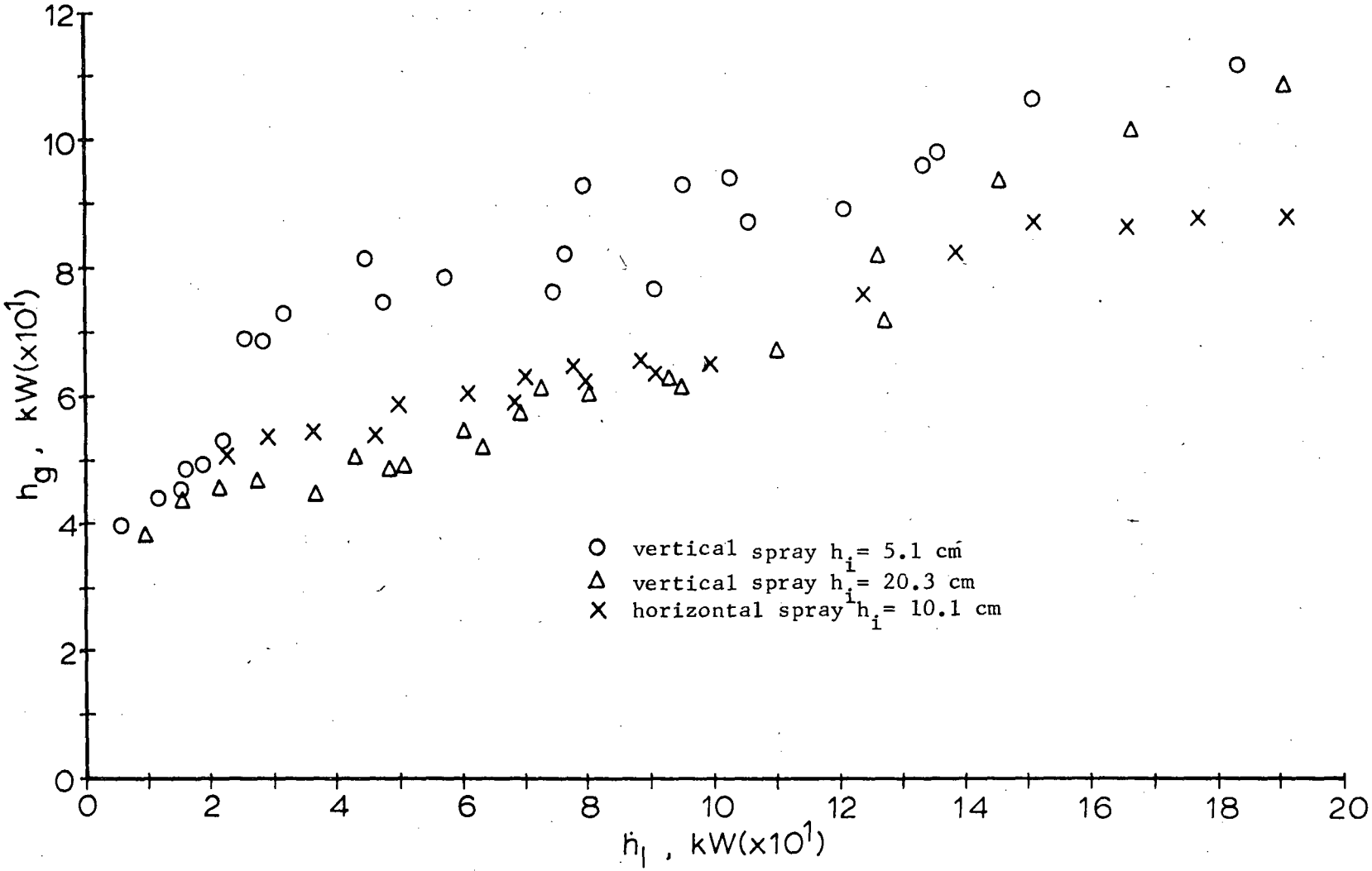

Fig. 8 Comparison of vertical and horizontal jet data.

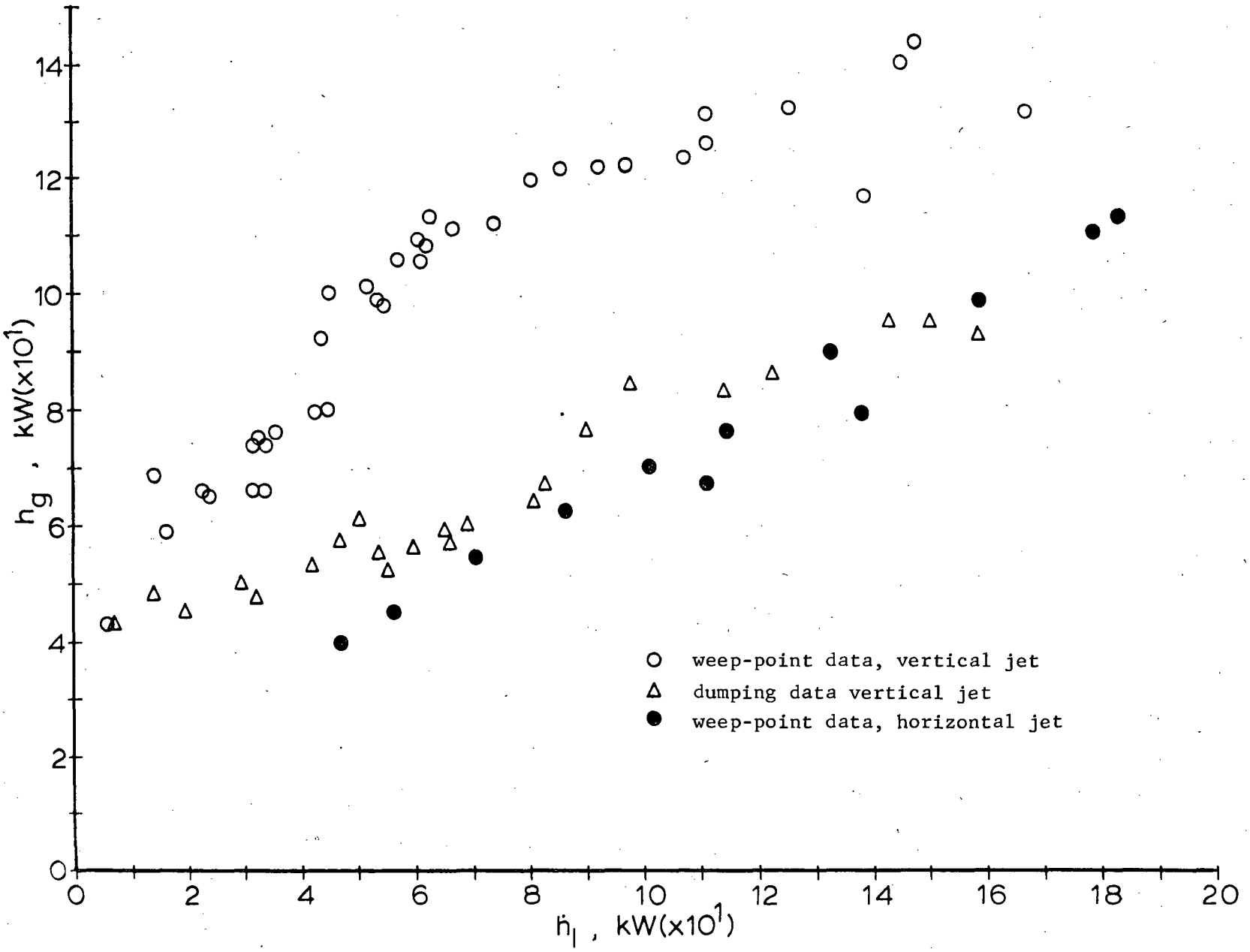

Fig. 9 The results of 0 cm injection and comparison to .5 cm horizontal jet data.

also noted that, the slope of the curve at high water enthalpy rates is the same as for the corresponding part of the 5.1 cm data. This implies that, after maximum mixing efficiency is reached, the flooding phenomenon is similar in each case.

An interesting observation is that the condensation rate is almost the same for the first two sets of data, namely 35.5 cm and 20 cm injection height data, and also for the parts of the last two sets of data (0 cm and 5 cm) after the deflection point. Since in both low injection height cases there is some water jet below the plate, the high condensation rate is expected. The deflection point is thought to be the point where maximum condensation rate for that portion of the spray below the plate has been reached. Beyond the deflection point, no more condensation is possible below the perforated plate, but there is some above the plate. This seems to be a physical explanation for the similar slopes in that region.

To observe the transition from the weep-point to dumping, some experiments were done with partial delivery for a fixed water flow rate and injection height point (.038 kg/sec and 20.3 cm see Fig. 10). For low water flow rate it was possible to get 90% delivery. However, it was not possible to obtain a similar curve for high flow rate conditions because at about 20% delivery, total dumping occurred. This discontinuity was also observed by Naitoh et al. (17), for flooding experiments above the upper tie plate of BWR fuel bundles. According to their observation, once subcooled water passes through the plate, it causes a decrease in the flow rate of ascending steam, which, in turn, causes more water to weep. This trend contiues until the dumping occurs. This is, of course, valid for high injection positions, where the jet cannot extend to the plate.

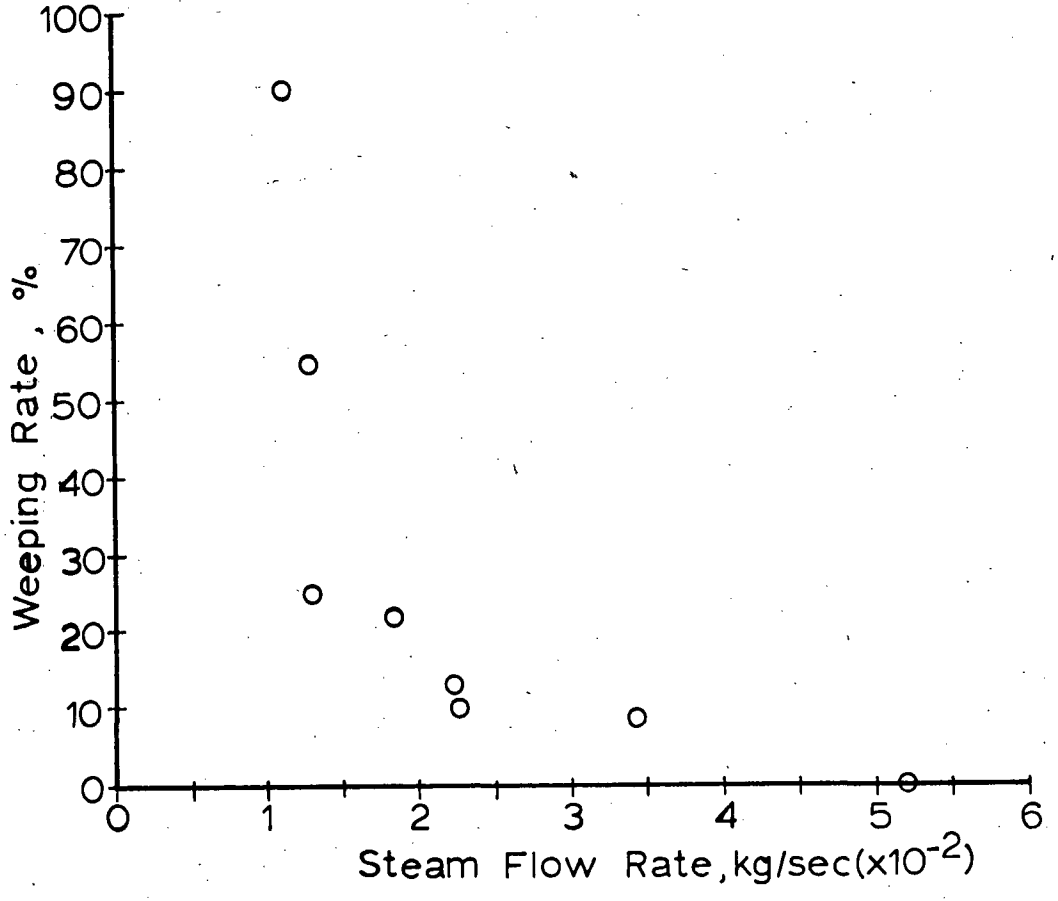

Fig. 10 Partial delivery data for h_i= 20.3 cm and water flow rate, w_f= kg/sec.

4.1.2. Further Investigations

A common behavior of all vertical injection data is that the dumping and the weep-point curves tend to intersect at high water enthalpy fluxes. From the experiments it has been observed that for the highest water flow rates tested, the flooding condition could switch from no weeping to dumping. Practically no partial delivery was observed. Instead, after total dumping occurred, the condition switched back to no-weeping for some tests. This is thought to be the point of intersection of the two curves, where the flow becomes unstable and switches back and forth between the two extreme conditions.

After the point where total condensation occurred inside the pool, an increase in water flow rate resulted in the decrease of average pool temperature. Actually, the temperature of the water just above the plate remained almost saturated until a critical range of water flow rate (near the intersection point mentioned above) was reached. As the decrease in the two-phase region inside the pool would imply, increasing water flow rate would move a "cold front" towards the plate. When this cold front reached the plate (i.e., when the total condensation occurred just above the plate) the phenomena became unstable (i.e., the intersection point was close).

In order to understand the total collapse of the water pool from no weeping condition at the highest flow rates tested, the critical degree of local subcooling was estimated based on the formula given by Merilo et al. (20). According to their study based on the results of Cumo et al. (21), the critical subcooling, ΔT_{sc} , where the nearly cylindrical vapor jet becomes unstable is given as:

$$\Delta T_{sc} \approx \frac{0.1\ \rho_g h_{fg}}{\rho_f C_p n K^*} \qquad (24)$$

This equation is valid for $x/d > 0.3$, where x is the axial distance, d is the vapor jet diameter and n is equal to -1/2. In deriving Eq. (24) d was taken to be in the order of 0.9D, D being the orifice (hole in this case) diameter. The single phase value of the turbulence constant K^* is 0.02. But Merilo et al. (20) observed that, based on their data, this value should be more nearly 0.002. When K^* is taken to be 0.002, ΔT_{sc} is found to be approximately 30^oC. In this study, it has been very difficult to accurately determine the temperature above the plate because the thermocouple was alternately exposed to both steam and water. However for low water injection heights, most of the inlet water is exposed to steam; the outlet water temperature is assumed to be pool temperature (measurements of the temperature above the plate for moderate flow rates confirmed this assumption). The temperatures were found to be between 67^oC and 85^oC for water flow rates ranging from 27.9 kg/min to 15.9 kg/min respectively (this being the highest range tested). Total collapse of the water pool above the plate occurred for the highest water flow rates, i.e., lowest temperatures. This can be attributed to the critical subcooling. The water temperature above the plate having reached some critical value, a sudden collapse of the steam might cause total dumping. However this investigation could be improved by taking more accurate measurements of the water temperature above the plate.

Looking at the other extreme, the lowest flow rates, the water jet was observed to break down at some point when the steam flow rate was increased from zero. A rough estimate of the wave length of interfacial instability (22) was made and was found to be in the same order of magnitude as the jet diameter, for the actual steam flow rates obtained from the experiments.

Furthermore, when the water droplets are approximated by solid spheres, an order of magnitude analysis reveals that the maximum size of the water droplets that can be carried by oncoming steam flow is the same as the jet diameter. Therefore the breakdown of the jet is expected, at least for small water flow rates.

4.1.3 Dimensionless Analysis

The weep point data were correlated by using Eq. (23) which is

$$H_{g,e}^{*\,1/2}/C = 1 \tag{23}$$

and C is calculated by

$$C = 1.07 + 4.33 \times 10^{-3} L^{*} \tag{14}$$

where

$$L^{*} = n\pi\, D_h [g(\rho_f - \rho_g)/\sigma]^{1/2} \tag{15}$$

For this case L^{*} equal to 197.7. Since Eq. (23) is valid for $30 < L^{*} < 200$, it can be used to correlate the data. Then the constant C is equal to 1.927. The dimensionless effective steam flow rate was defined as:

$$H_{g,e}^{*} = H_{g}^{*} - f[C_p(T_{s,f} - T_f)/h_{fg}](\rho_f/\rho_g)^{1/2}\, H_{f,in}^{*} \tag{21}$$

where

$$H^*_{g,f} = [\rho_{g,f}/gw(\rho_f - \rho_g)]^{1/2} j_{g,f} \tag{11}$$

and

$$w = D_h^{(1-\alpha)} [\sigma/g(\rho_f - \rho_g)]^{\alpha/2} \tag{12}$$

The value of the constant α, for 15 hole plate, is 0.884, and the volumetric flux, $j_{g,f}$, is given by

$$j_{g,f} = W_{g,f}/\rho_{g,f} A_h \tag{25}$$

where A_h is the total area of the holes.

In Eq. (21), everything is known except the condensation efficiency f, which is empirically obtained from enthalpy flux curves. For 35.6 cm and 20.3 cm injection height data, the curves are simple and the slopes are found to be 0.25 and 0.27 respectively. Using this result, the dimensionless effective steam flow rate, $H^*_{g,e}$ are calculated and the values of $H^{1/2}_{g,e}/C$ corresponding to the weep-point data of these inlet positions are plotted in Fig. 11a. According to Eq. (23), the result is expected to be constant and equal to one. But the constant line is observed to be slightly lower than $H^{*\,1/2}_{g,e}/C = 1$ line, for both sets of data. This difference is thought to be due to the criterion to determine the weep-point, where actually a small amount of water is allowed to weep through the perforated plate. Even though the weeping rate of water was kept within a few percent of the inlet water

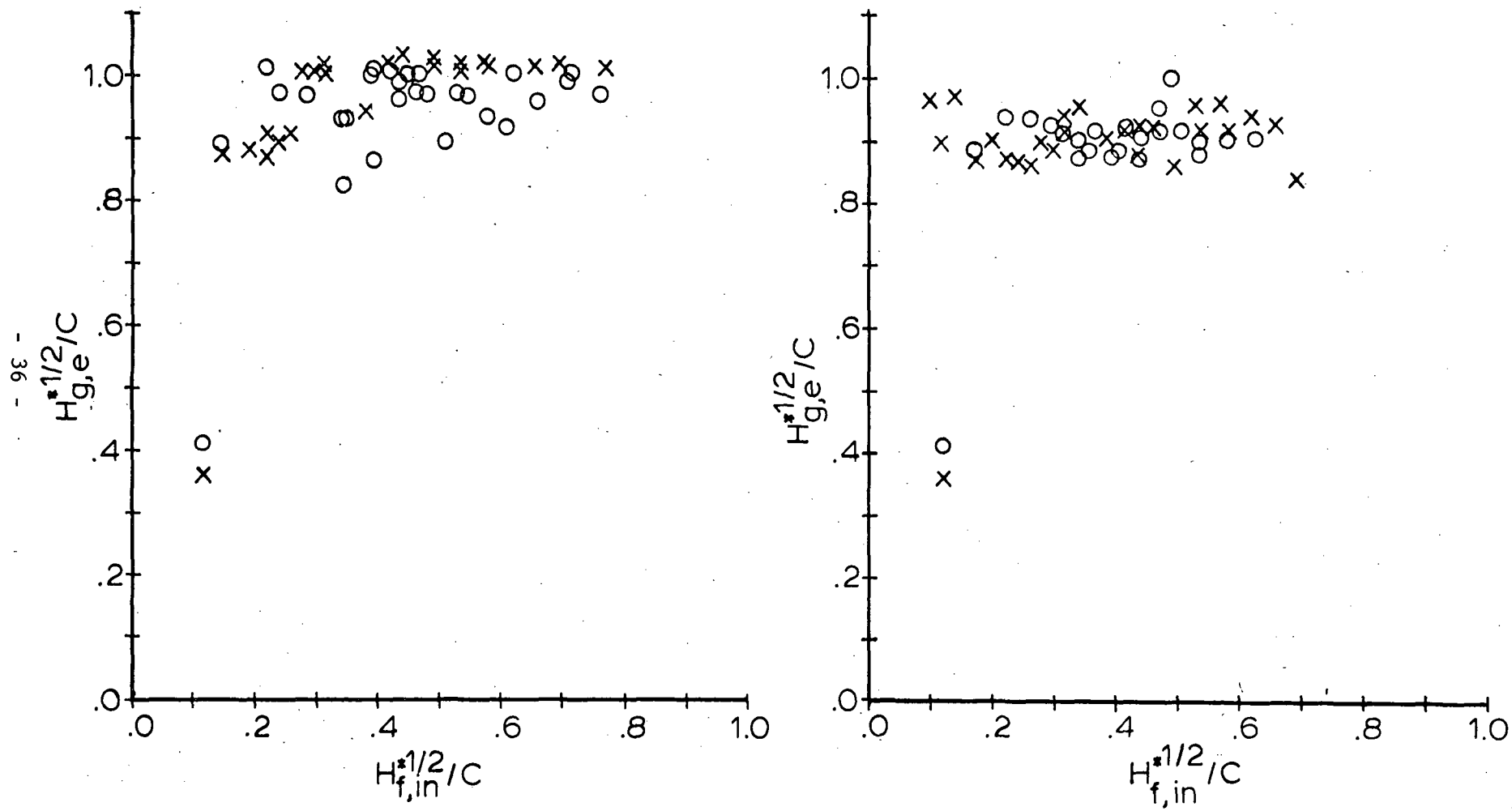

a) low injection height data

b) high injection height data

Fig. 11 The dimensionless effective steam flow rate for the weep-point data.

flow rate, referring to Fig. 10, the change in steam flow rate can be somewhat significant. Therefore, it can be expected to yield a low value for $H^*_{g,e}$.

The calcultion of the condensation efficiency, f, for high injection height data was rather simple. However, for low injection height data, the slopes of the curves for the weep-point data are not constant. Hence, each curve is approximated by two straight lines with different slopes, f_1 and f_2. Therefore, the dimensionless effective steam flow rate is corrected to correlate these data. For the first part of the curves, with slope f_1, the original equation is still applicable. For the second part of the curves, with slope f_2, the following equation is used:

$$H^*_{g,e} = H^*_g - f_1(I\ H^*_{f,in})_i - f_2 I[H^*_{f,in} - (H^*_{f,in})_i] \qquad (26)$$

where

$$I = [C_p(T_{sat} - t_f)/h_{fg}](\rho_f/\rho_g)^{1/2} \qquad (27)$$

and the parameters with subscripts i are evaluated at the intersection point of the two straight lines with slopes f_1 and f_2. The other terms are evaluated at the point of interest. The term $f_1(I\ H^*_{f,in})_i$ is the correction for the amount of steam condensed up to the intersection point and the term $f_2[I(H^*_{f,in} - (H^*_{f,in})_i)]$ is the correction for the amount of steam condensed from the intersection point up to the point of interest. The point of intersection is empirically determined. The results are shown in Fig. 11a. The data, especially for 5.1 cm injection height is scattered because of the unstable behavior of the experiments for low injection heights. But, in general, the same behavior as for the high injection height data is observed.

The effective steam flow rate was also calculated for total dumping data. Since all the dumping curves are straight lines, the original definition of $H^*_{g,e}$ is used and the values of $H^{*\,1/2}_{g,e}/C$ are plotted in Figs. 12a and 12b. The data for each injection point can be approximated as constant; but in this case, the value of the constant is much lower than the weep-point data (Figs. 11a and 11b).

If the dumping data are thought to correspond to the condition just before total dumping occurs, Eq. (16) can be applied to these data:

$$H^{*\,1/2}_{g,e}/C + H^*_{f,d}/C = 1 \qquad (16)$$

But $H^{*\,1/2}_{g,e}/C$ is approximately equal to a constant (0.7 for 35.6 cm injection height data (Fig. 12a)). This implies that the dimensionless water delivery rate, $H^*_{g,d}$ is also constant. That is, the amount of water delivery just before dumping occurs is independent of the inlet water flow rate.

It is also observed that the value of $H^{*\,1/2}_{g,e}/C$ decreases as the water inlet is lowered. Therefore, the water inlet position does affect the amount of water delivered through the perforated plate at dumping point. The lower the water injection height, the higher the water delivery rate. If the water delivery rate could have been accurately measured, the compatibility of Eq. (16) for the dumping data could have been determined.

4.2 Effects of Unheated Block Below Perforated Plate

The effects of the block have been tested with 15 hole plate (Fig. 2a) and vertical water spray. Data were taken for two different positions of the block; namely, 1.9 cm and 5.7 cm below the test plate. The open flow area of the block corresponds to a 9 hole perforated plate. Two different water inlet

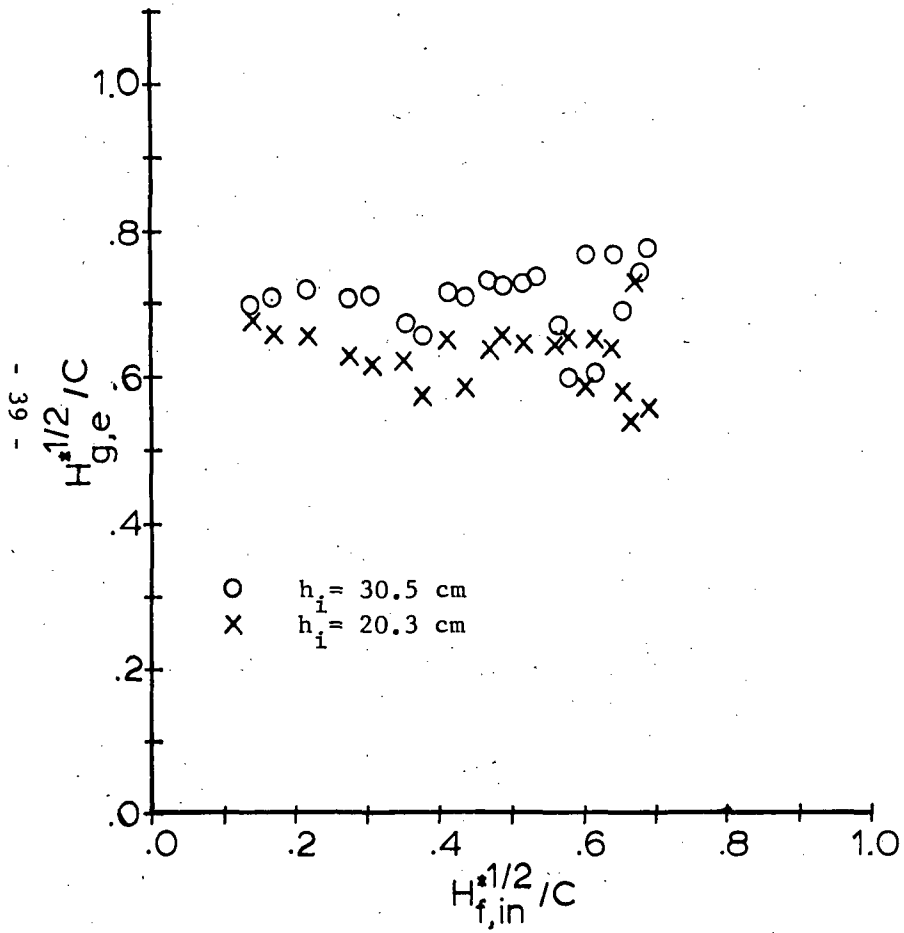

a) high injection height data

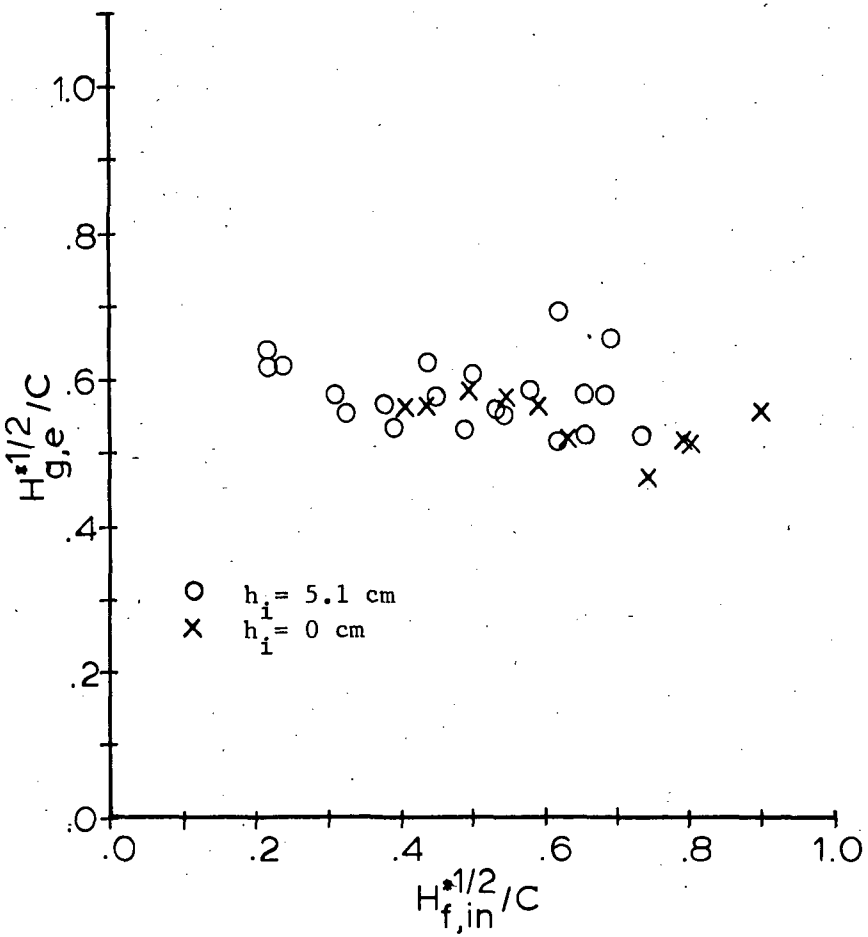

b) low injection height data

Fig. 12 The dimensionless effective steam flow rate for total dumping data.

positions; namely, 20.3 cm and 5.1 cm above the perforated plates, were examined which corresponded to high and low injection height cases. The results for the 20.3 cm injection height data, together with the data obtained without the block, are shown in Fig. 13. It is observed that the position of the block does not make any difference. But its presence has an effect. The steam flow rate is lower in this case, but the slope is higher. At 20.3 cm injection height there is no water jet below the perforated plate. The weeping water is trapped by the block. Since it has an open flow area which is less than that of the perforated plate (9 hole compared to 15 hole) the volumetric flux, j_{gh}, through the block is higher than that through the plate. Therefore, the water that weeps from the plate is prevented by the block from reaching the bottom of the channel, which was the criterion to determine the weep-point.

In the case of 5.1 cm water injection height it is observed that the position of the block has an effect on the weep-point (Fig. 14). The lowest steam enthalpy fluxes are obtained for the position of the block at 5.7 cm and the highests are obtained for the data without the block. The water jet did not reach the block when the block was 5.7 cm below the perforated plate. Steam condensation occurs between the block and the perforated plate. For this situation, the weeping phenomenon occurs mostly between the block and the perforated plate. These data are similar to low injection height, horizontal spray data with a 9 hole perforated plate. However, when the block is placed at 1.9 cm below the perforated plate, the water spray strikes the block and the water appears to spread in the small volume between the block and the perforated plate. This increases the mixing efficiency; therefore causing more condensation, which results in higher steam flow rates.

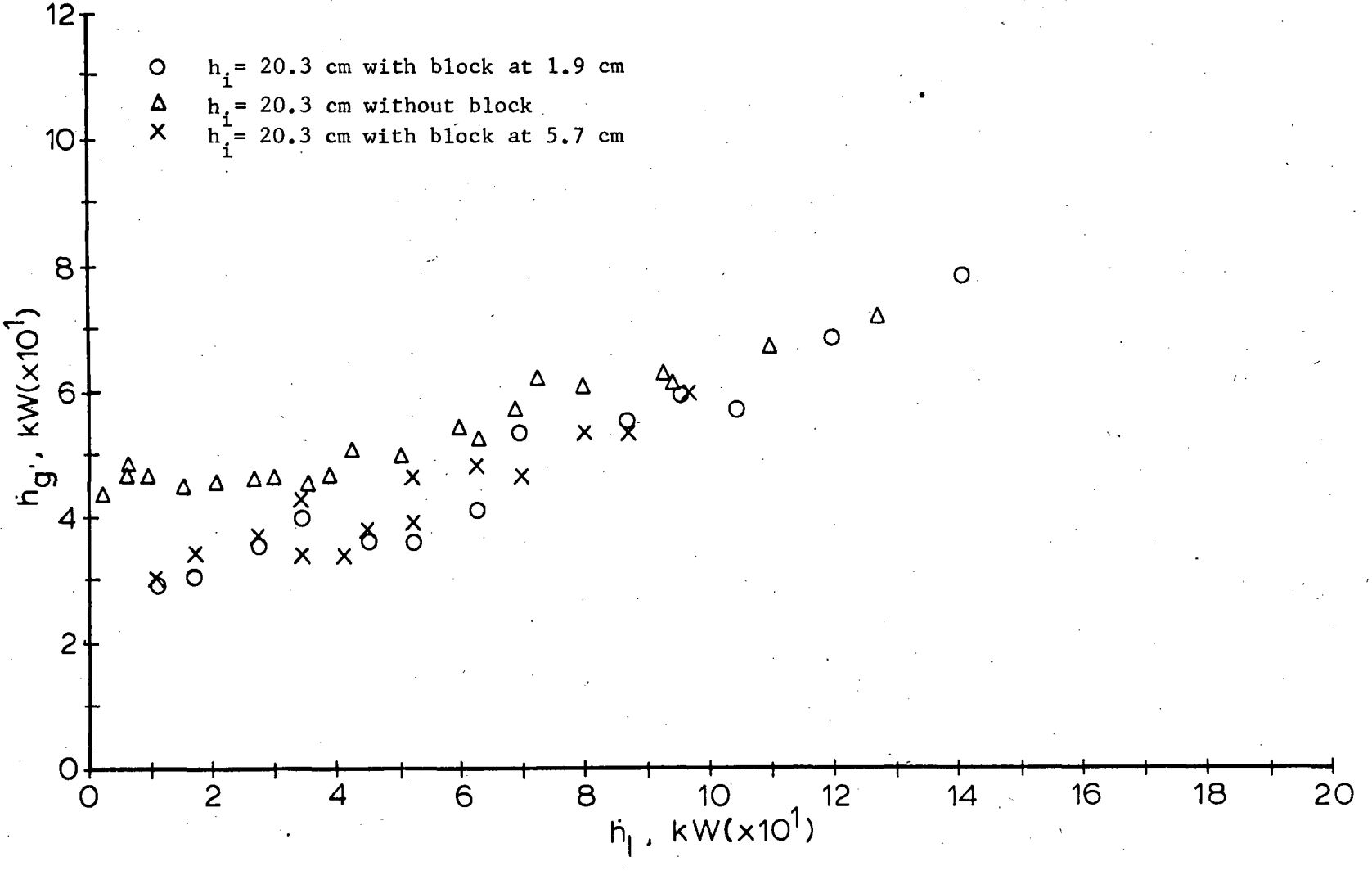

Fig. 13 Weep-point data with block and comparison to data without block (15 hole plate).

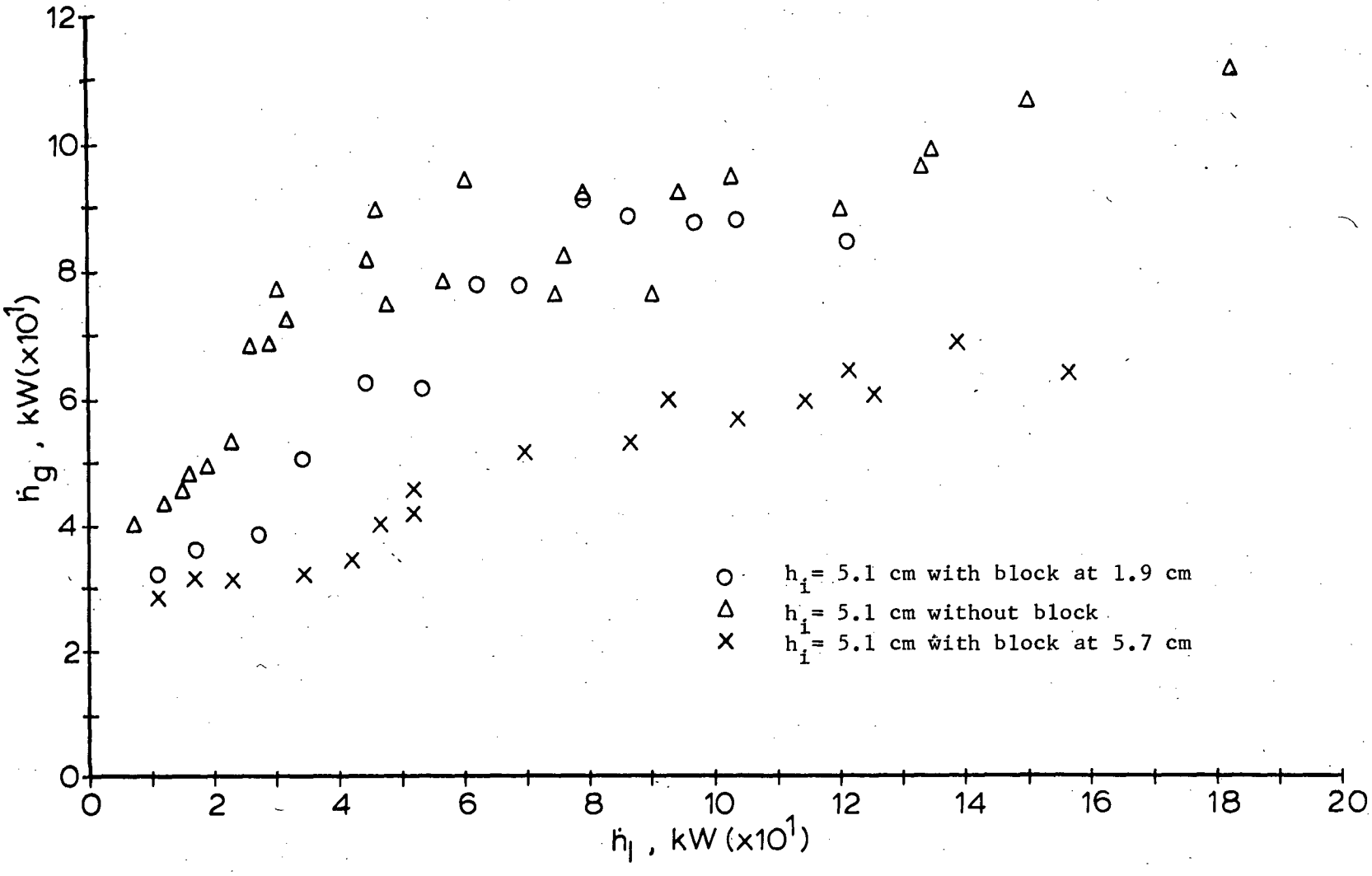

Fig. 14 Weep-point data with block for low injection (15 hole plate).

As a final test, the 9 hole plate (Fig. 2b) and the horizontal spray injector have been used with the block being fixed at 5.7 cm below the test plate. The injector has been placed at 20.3 cm and 35.5 cm heights above the perforated plate and the results have been compared to C. L. Hsieh's data (5) taken with the same plate and injector, but without the block (Fig. 15). As expected, the position of the injector at these large heights, does not have any effect on weeping phenomenon with the block. However, they both are similar in magnitudes to Hsieh's low injection height data, but similar slopes to Hsieh's high height injection data. The cause might be two-fold.

First, a major cause is thought to be due to the different criteria used for determining the weep-point. A more careful examination is worthwhile to understand the two criteria. In the case of Hsieh's high injection height data (Fig. 15, h_{in} = 30.5 cm) which was obtained with horizontal water spray and without the block, the temperature of the water just above the plate was essentially saturated. Therefore it can be assumed that there is practically no condensation at or near the holes of the plate. Hence, those data correspond to the lowest steam enthalpy fluxes. On the other hand, the perforation ratio of the 9 hole plate being 0.254, the steam velocity through the holes is almost 4 times larger than the steam velocity below the plate. Therefore once water weeps through the perforated plate it implies that steam flow through the holes is not high enough to suspend the water droplets. Once the droplets pass through the holes, the steam velocity below the plate being much lower, the droplets continue to fall (this is the downward delivery point). However, when the water inlet height is lowered (Fig.15 h_i = 10.1 cm) the temperature just above the plate is subcooled. Therefore, condensation occurs at or near the holes. The condensation of steam in the holes entrains water through the holes. Hence, weeping occurs due to the condensation. The water droplets

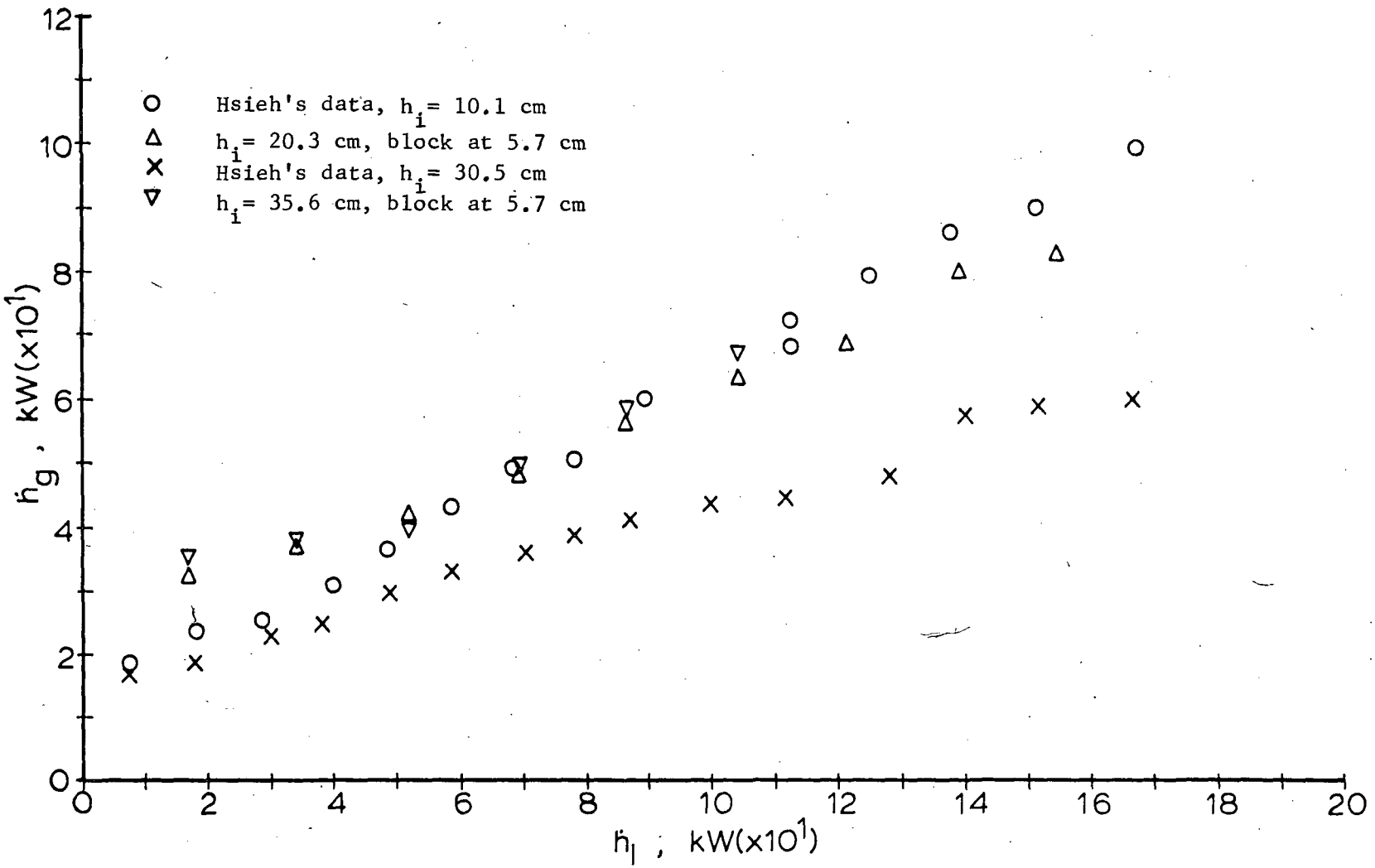

Fig. 15 Weep-point data with 9 hole plate and comparison to Hsieh data.

that penetrate below the perforated plate are turned around and blown back, because the steam flow rate is sufficiently high (this is the turn-around point). Weeping from the perforated plate is due to condensation, but the water droplets cannot reach the bottom of the channel. Thus, for high injection heights above the plate, the water pool is saturated, downwards delivery and the turn-around points are the same. However for low injection heights, when the steam flow rate is increased from a partial delivery state, the downwards delivery point is reached. Further increase of the steam flow rate and the turn-around point is reached.

In Fig. 15, it is seen that the magnitude of steam enthalpy flux for high injection height data with the block is the same as for the low injection height data without the block. Although the injection height was high and the pool temperature was near saturation, the turn-around phenomenon has been observed in the experiments with the block. It is believed the existence of this phenomenon in the case of no condensation near the perforated plate is due to the presence of the block. The steam velocity profile below the perforated plate is determined by the block. Some holes in the perforation plate are subject to velocities low enough to permit weeping. However, the droplets encounter the high steam velocity issuing above the block which blows the droplets back. Thus, the turn-around point is obtained and not the downwards delivery point. It is also noted that the slope of this curve is the same as the Hsieh's high injection height data even though the magnitude of steam enthalpy flux is larger. This confirms that there is no condensation in or near the holes with or without the block for high injection positions.

5. Conclusions

From the experiments with a vertical injector, it has been found that, for high water inlet heights, the effective jet length cannot extend to the perforated plate. No difference was observed between horizontal spray data and vertical spray data on the weep-point and the total dumping point. On the other hand, when the water inlet height above the perforated plate is 5.1 cm or less, the effective water jet length extends to the perforated plate and causes higher condensation efficiencies. Since some steam is condensed below the plate, a considerable increase in steam flow rate is observed for the weep-point data. However, the dumping data are not much affected. As a result, the enthalpy flux curves of total dumping are similar for different inlet heights.

The dumping phenomenon is observed to be related to the average subcooling temperature of the water pool above the plate. Steam bubbles collapse on the holes of the perforated plate for a critical subcooling temperature, causing total collapse of the water pool above the plate. This phenomenon can occur even for no-weeping conditions if the water flow rate is sufficiently high to bring the pool temperature to the critical subcooling temperature. The no-weeping condition then suddenly changes to total dumping. However, more detailed investigations are necessary to estimate the critical degree of subcooling or the corresponding water flow rate, for this specific flow.

The dimensionless effective steam flow rate defined for horizontal spray data correlates the vertical water spray data for high injection heights only. For low injection heights, two different formulas are used for correlation, because two different condensation efficiencies have been observed. For low water enthalpy fluxes, the original formula is used. The

condensation efficiency is determined from the slope of the corresponding portion of the enthalpy flux curves. For higher water enthalpy fluxes, the formula has been adjusted for the change of the slope of the enthalpy flux curves. The results are found to be independent of the water inlet height. This analysis is valid only for the weep-point data. In the case of total dumping, the original dimensionless parameter correlated all the data. It is found that the effective dimensionless steam flow rate is independent of inlet water flow rate. If the dimensionless analysis is assumed to be valid for the point just before dumping, the sum of the effective steam flow rate and water delivery rate is constant. Therefore, water delivery rate is also independent of inlet water flow rate. This implies that the amount of water weeping just before the total dumping occurs is always the same. However this result needs further verification by more accurate measurement of the water delivery rate.

When an unheated block is placed below the plate, the change of steam flow pattern affects the weeping phenomenon. If the open flow area of the block is less than that of the plate the steam flow rate is observed to be slightly lower for high water injection. But for low injection, the choking occurs at the block instead of the plate. When the open flow area is the same for both the block and the plate, horizontal spray experiments for high injection heights reveal that the steam flow rates required to keep water from weeping are higher compared to those obtained in the experiment without the block.

REFERENCES:

(1) Bulletin HY-30,Hy-Park Packings, Norton Co., (1977).

(2) Sherwood, T. K., et al., "Mass Transfer", pp. 599-603, McGraw-Hill, Inc., NY (1975).

(3) Wallis, G. B., et al., "Analysis of ECC Delivery", CREARE TN-231 (176).

(4) Ueda, T. and S. Suzuki, "Behavior of Liquid Films and Flooding in Counter-Current Two Phase Flow. Part 2. Flow in Annuli and Rod Bundles", Int. J. Multiphase Flow, 4 pp. 157-170 (1978).

(5) Hsieh, C. L., "Counter-Current Air/Water and Steam/Water Flow Above A Perforated Plate", Dissertation submitted to Northwestern University Graduate School (1979).

(6) Mayfield, F. D., et al., "Perforated Plate Distillation Columns", Ind. Eng. Chem., 44 9, pp. 2238-2249 (Sept. 1952).

(7) Arnold, D. S., et al., "Performance of Perforated-Plate Distillation Columns", Chem. Eng. Prog., 48, 12, pp. 663-642 (1952).

(8) Zenz, F. A., "How to Calculate Capacities of Perforated-Plates", Petroleum Refiner, 33, 2, pp. 99-102 (Feb. 1954).

(9) Jones, D. D., "Subcooled Counter-Current Flow Limiting Characteristics of the Upper Region of a BWR Fuel Bundle", General Electric Company, Nuclear Systems Products Division, BD/ECC Program, NEDG-NUREG-25549 (1977).

(10) Sun, K. H. and R. T. Fernandez, "Counter-Current Flow Limitation Correlation for BWR Bundles During LOCA", ANS Transactions, 27, pp. 605 (1977).

(11) Wallis, G. B., "One-Dimensional Two-Phase Flow", McGraw-Hill, Inc., NY (1969).

(12) Pushkina, O. L. and Y. L. Sorokin, "Breakdown of Liquid Film Motion in Vertical Tubes", Heat Transfer-Soviet Research, 1, 5, pp. 56 (1969).

(13) Block, J. A. and V. E.Schrock, "Emergency Cooling Water Delivery to the Core Inlet of PWRs During LOCA", published in the symposium on Thermal Hydrolic Aspects of Nuclear Reactor Safety, ASME Winter Annual Meeting, (1977).

(14) Wallis, G. B. and S. Makkenchery, "The Hanging Film Phenomena in Vertical Annular Two-Phase Flow", ASME Journal of Fluids Engineering, pp. 297-298 (Sept. 1974).

(15) Hsu, Y. Y. and R. W. Graham, "Transport Processes in Boiling and Two-Phase Systems", McGraw-Hill, Inc., NY (1976).

(16) Punches, W. C., "MAYU04, A Method to Evaluate Transient Thermal Hydrolic Conditions in Rod Bundles", GEAP-23517, General Electric Co., Nuclear Energy Division, (Mar. 1977).

(17) Naitoh, M., K. Chino and R. Kawabe, "Restrictive Effect of Ascending Steam on Falling Water During Top Spray Emergency Core Cooling", Journal of Nuclear Science and Technology, 15, 11, pp. 806 (1978).

(18) Jacoby, J. K., et al., "Quick Look Report on KUU Support Column Air/Water Experiments", EG and G Report, RDW-23-78 (1978).

(19) Block, J. A. and H. Rothe, "Progress on ECC By-Pass Scaling", CREARE TN-272, NUREG/CR-0048, R-2 (1977).*

(20) Merilo, M., M. Colah, R. B. Duffey, "The Condensation Induced Transition From Bubbling to Liquid Downflow in A Turbulent Two-Phase Pool", ASME, Nonequilibrium Interfacial Transport Process, p. 53 (1979).

*Available for purchase from the NRC/GPO Sales Program, U.S. Nuclear Regulatory Commission, Washington, DC 20555 and/or the National Technical Information Service, Springfield, VA 22161.

(21) Cumo, M., Farello, G. E., and Ferrari, G., "Heat Transfer in Condensing Jets of Steam Water", Proc. Sixth Int. Heat Transfer Conference, Toronto, 5, pp. 101-106 (1978) (also CNEN Report RT/ING(77)8).

(22) Bankoff, S. G., "Interfacial Instability: Theory and Applications", presented at 1979-1980 Lecture Series Programme, von Karman Institute for Fluid Dynamics (1980).

NRC FORM 335 (7-77) U.S. NUCLEAR REGULATORY COMMISSION

BIBLIOGRAPHIC DATA SHEET

1. REPORT NUMBER (Assigned by DDC): NUREG/CR-2323

4. TITLE AND SUBTITLE (Add Volume No., if appropriate): Countercurrent Steam/Water Flow Above a Perforated Plate-Vertical Injection of Water

2. (Leave blank)

3. RECIPIENT'S ACCESSION NO.

7. AUTHOR(S): I. Dilber, S. G. Bankoff, R. S. Tankin, M. C. Yuen

5. DATE REPORT COMPLETED: MONTH July, YEAR 1981

9. PERFORMING ORGANIZATION NAME AND MAILING ADDRESS (Include Zip Code)
Northwestern University
Department of Chemical Engineering
Department of Mechanical and Nuclear Engineering
Evanston, IL 60201

DATE REPORT ISSUED: MONTH September, YEAR 1981

6. (Leave blank)

8. (Leave blank)

12. SPONSORING ORGANIZATION NAME AND MAILING ADDRESS (Include Zip Code)
U. S. Nuclear Regulatory Commission
Office of Nuclear Regulatory Research
Division of Accident Evaluation
Washington, D. C. 20555

10. PROJECT/TASK/WORK UNIT NO.

11. CONTRACT NO.: FIN B6188

13. TYPE OF REPORT: Topical

PERIOD COVERED (Inclusive dates): August 1980 - July 1981

15. SUPPLEMENTARY NOTES

14. (Leave blank)

16. ABSTRACT (200 words or less)

Countercurrent flow limiting phenomenon above a perforated plate has been studied in a steam/water environment. Water was injected as a vertical jet and the injection height above the perforated plate was changed from 0 cm to 35.6 cm. The 15 hole perforated plate has a rectangular cross section with a perforation ratio of 0.423. The weep-points and total dumping points have been determined for low and high water injection heights above the perforated plate and the results have been compared to those of the horizontal water spray experiments. The data corresponding to high water injection heights were similar to those of the horizontal water spray experiments. However a different behavior was observed for the weep-point data with low water inlet heights. The dumping point was little affected by the water inlet position above the perforated plate. The dimensionless effective steam flow rate defined for the experiments with horizontal water spray was used to correlate the data corresponding to both the onset of weeping and the total dumping points. The correlation was successful for the weep-point data with high water injection heights. However the dimensionless parameter was redefined for the weeping-point data with low water injection heights.

17. KEY WORDS AND DOCUMENT ANALYSIS

17a. DESCRIPTORS

Steam/Water Environment
Countercurrent Flow
Core Spray

17b. IDENTIFIERS/OPEN-ENDED TERMS

18. AVAILABILITY STATEMENT: Unlimited

19. SECURITY CLASS (This report): Unclassified

21. NO. OF PAGES

20. SECURITY CLASS (This page): Unclassified

22. PRICE: $

NRC FORM 335 (7-77)

NUREG/CR-2323

COUNTERCURRENT STEAM/WATER FLOW ABOVE A PERFORATED PLATE-VERTICAL INJECTION OF WATER

SEPTEMBER 1981